affects the eradication of HCV by IFN-based therapy in patients chronically infected with the virus.[5,6]

In this study, we evaluated the anti-HCV effects of vitamin D_3 and its metabolites, $25(OH)D_3$, $1,25(OH)_2D_3$, and $24,25(OH)_2D_3$. Here we show that $25(OH)D_3$, but not $1,25(OH)_2D_3$, possesses an anti-HCV effect targeting the assembly of the infectious virus. This finding suggests the novel conjunctive role of $25(OH)D_3$ in IFN-based therapy against chronic hepatitis C.

Materials and Methods

Cell Culture and Reagents. The human hepatoma cell line, HuH-7, and its derivative cell line, Huh-7.5.1, provided by Francis Chisari (Scripps Research Institute, La Jolla, CA) were maintained at 37°C, 5% CO_2 in Dulbecco's modified Eagle's medium (DMEM), containing 10% fetal bovine serum. The HuH-7 derivative cell line Huh7-25, which lacks CD81 expression,[14] was also used.

Vitamin D_3 and $24,25(OH)_2D_3$ were purchased from Enzo Life Sciences Inc. (Farmingdale, NY). $25(OH)D_3$ was obtained from Immundiagnostik AG (Bensheim, Germany). $1,25(OH)_2D_3$ was kindly provided by Chugai Pharmaceutical Co. Ltd. (Tokyo, Japan). Vitamin D_3 and its metabolites were dissolved in ethanol at the stock concentration of 2.0 mM, and stored at −30°C or −80°C until use. Only glass- or Teflon-made wares were used for handling ethanol solutions of vitamin D_3 and its metabolites.

Human IFN-alfa2b was obtained from MSD K.K. (Tokyo, Japan).

Cell Culture–Generated HCV. The production of cell culture–generated HCV JFH-1 virus (HCVcc) has been reported.[15] Briefly, the plasmid pJFH-1 was linearized at the 3′ end of the full-genome JFH-1 complementary DNA by XbaI digestion. Digested plasmid DNA was purified and used as a template for *in vitro* RNA synthesis with a MEGAscript T7 kit (Ambion, Austin, TX). Synthesized full-length JFH-1 RNA was electroporated into Huh-7.5.1 cells with cytomix as described. After long-term culture of transfected cells, cell culture–adapted HCVcc was harvested and stocked for further infection studies (Kato et al., unpublished data).

Quantification of HCV RNA, Core Antigen, and Cell Viability. Total RNA was extracted from 140 μL of culture medium with the QIAamp Viral RNA kit (QIAGEN, Valencia, CA) or from harvested cell pellets with the RNeasy mini kit (QIAGEN). Real-time quantitative reverse-transcription polymerase chain reaction (PCR) was performed to determine the copy number of HCV RNA as described.[16] The concentration of total RNA in the cells was determined using a Nanodrop Spectrophotometer ND-1000 (Thermo Scientific, Rockford, IL). The concentration of HCV core antigen (Ag) in filtered culture medium and cell lysates was determined using the Lumipulse Ortho HCV Ag kit (Ortho Clinical Diagnostics, Tokyo, Japan) as described.[17]

To assess cell viability, a water-soluble tetrazolium salt, 2-(2-methoxy-4- nitrophenyl)-3-(4-nitrophenyl)-5-(2,4-disulfophenyl)-2H tetrazolium, monosodium salt (WST-8) was used as an indicator.[18] In brief, the WST-8 reagent solution (10 μL) was added to each well of a 96-well microplate containing 100 μL of cells in the culture medium. The plate was incubated for 1 hour at 37°C, and the absorbance in each well was measured at 450 nm using a microplate reader.

HCV Pseudoparticles Assay. HCV pseudoparticles (HCVpp) harboring E1 and E2 glycoproteins of various HCV clones (H77, genotype 1a; TH, genotype 1b; JFH-1, genotype 2a; and J6CF, genotype 2a) or vesicular stomatitis virus G envelope glycoprotein were produced as described.[19,20] Briefly, to generate HCVpp, the glycoprotein-expressing vector, the gag-pol expression vector encoding murine leukemia virus (MLV) retroviral cores, and the MLV-derived transfer vector encoding the luciferase reporter protein were transfected using FuGENE6 (Roche, Indianapolis, IN) into 2.5×10^6 293T cells seeded in 10 cm dish 1 day earlier. The medium was replaced with fresh complete DMEM 6 hours after transfection. Supernatants containing the HCVpp were harvested 48 hours later, cleared by passage through 0.45-μM pore-size filters, and used for infection assays. The target Huh-7.5.1 cells were seeded in 12-well plates at a density of 5×10^4 cells per well, incubated overnight at 37°C, and infected with the HCVpp in the presence of $25(OH)D_3$ or ethanol. At 16 hours postinfection,

Address reprint requests to: Takanobu Kato, M.D., Ph.D., Department of Virology II, National Institute of Infectious Diseases, Toyama 1-23-1, Shinjuku-ku, Tokyo 162-8640, Japan. E-mail: takato@nih.go.jp or Michio Imawari, M.D., Ph.D., Division of Gastroenterology, Department of Medicine, Showa University School of Medicine, 1-5-8 Hatanodai, Shinagawa-ku, Tokyo 142-8666, Japan. E-mail: imawari@med.showa-u.ac.jp.

View this article online at wileyonlinelibrary.com.

DOI 10.1002/hep.25763

Potential conflict of interest: Nothing to report.

Additional Supporting Information may be found in the online version of this article.

medium was replaced with DMEM with 10% fetal bovine serum, and cells were harvested 24 hours later for analysis of luciferase activity.

HCV Subgenomic Replicon Assay. The transient assay of the genotype 2a (JFH-1) subgenomic reporter replicon has been reported.[21] This subgenomic replicon contains the firefly luciferase reporter gene and enables assessment of HCV replication by measuring the luciferase activities in culture cells. Four hours after transfection, the cells in a portion of the plates were harvested as a control for transfection efficiency, and a remaining portion was treated with 25(OH)D_3 or ethanol. The cells were harvested 72 hours after transfection for luciferase measurement. Replication efficiency of HCV in each preparation was calculated as the percent of luciferase activity under the ethanol treatment after normalization by transfection efficiency.

Titration of HCV Infectivity. Culture medium was diluted 10-fold with phosphate-buffered saline and concentrated with Amicon Ultra-15 centrifugal filter units (Millipore, Billerica, MA) to avoid carrying over the test substances. Prepared samples were serially diluted in five-fold increments in complete DMEM and used to infect naïve Huh-7.5.1 cells seeded 24 hours earlier in poly-D-lysine–coated flat-bottom 96-well plates (Corning Inc., Corning, NY) at a density of 1×10^4 cells per well. Three days after infection, HCV-positive cells were detected with mouse monoclonal antibody recognizing the core protein (clone 2H9)[15] and visualized with Alexa Fluor 488 anti-mouse secondary antibody (Invitrogen). The infectivity titer was expressed as focus-forming units per milliliter supernatant (ffu/mL), expressing the mean number of HCV core–positive foci detected at the highest dilutions.[22] The intracellular infectivity and specific intracellular infectivity titer were determined as described.[23]

Isolation of a 25(OH)D_3-Resistant Mutant. In order to obtain a resistant mutant for 25(OH)D_3, the serial passage of JFH-1–transfected cells was performed. HuH-7 cells were electroporated with 3 μg of synthetic HCV RNA, resuspended in 10 mL of complete growth medium, and seeded into a 10-cm dish. After 24 hours, transfected cells were cultured with medium containing 1.0 μM of 25(OH)D_3. HCV titer was monitored by measuring the HCV core Ag, and the resistant mutant virus was harvested and stocked at the peak of the core Ag expression. HCV RNA was extracted from culture medium at this point, and complementary DNA was synthesized and amplified via nested PCR covering almost the entire open reading frame and part of the 5′ untranslated region as described.[23]

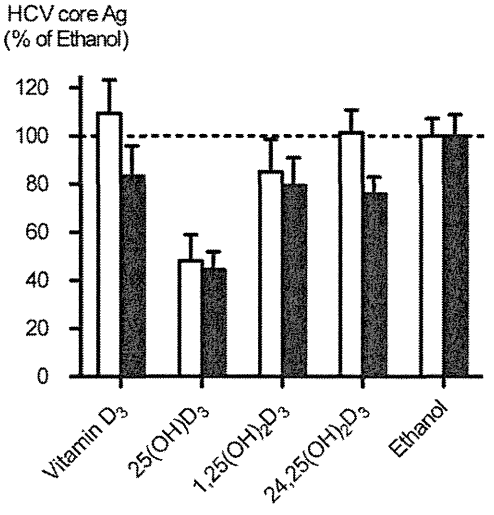

Fig. 1. Anti-HCV effect of vitamin D_3 and its metabolites. HuH-7 cells were pretreated with vitamin D_3, its metabolites, or ethanol (solvent control) and inoculated with HCVcc. HCV production was assessed by measuring the HCV core Ag after a 3-day treatment. HCV core Ag in culture medium and cell lysates are indicated by white and black bars, respectively. Results are expressed as the mean ± SD of the percent of the control (ethanol treatment).

Statistical Analysis. Assays were performed in triplicate. Data from repeated experiments are expressed as the mean ± SD. Statistical analysis was performed using the Student t test, and $P < 0.05$ was considered statistically significant.

Results

Anti-HCV Effect of 25(OH)D_3. To assess the anti-HCV effects of vitamin D_3 and its metabolites—25(OH)D_3, 1,25(OH)$_2$ D_3, and 24,25(OH)$_2D_3$—the HCVcc system was exploited. HuH-7 cells were treated with vitamin D_3 and its metabolites at a concentration of 1.0 μM and were infected with cell culture–adapted HCVcc at a multiplicity of infection of 0.5. Treatment with 25(OH)D_3 markedly reduces HCV core Ag levels in culture medium and cell lysate to 47.97 ± 10.89% and 44.39 ± 7.52% of the control levels, respectively (Fig. 1). Treatment with vitamin D_3 and 1,25(OH)$_2$ D_3 have no remarkable effects. The anti-HCV effect of 25(OH)D_3 on the core Ag is concentration-dependent from 0.125 to 1.0 μM (Fig. 2A). The calculated 50% effective concentration (EC_{50}) of core Ag in culture medium is 0.95 μM. A similar inhibitory effect was also observed for the HCV RNA titer (Fig. 2B). At the higher concentrations of 5 μM, 25(OH)D_3 reduced HCV core Ag levels to 0.4-1.8 % of control (Supporting Fig. 1A). WST-8 assay demonstrated no cytotoxicity in the cells treated with 25(OH)D_3 at a concentration of up

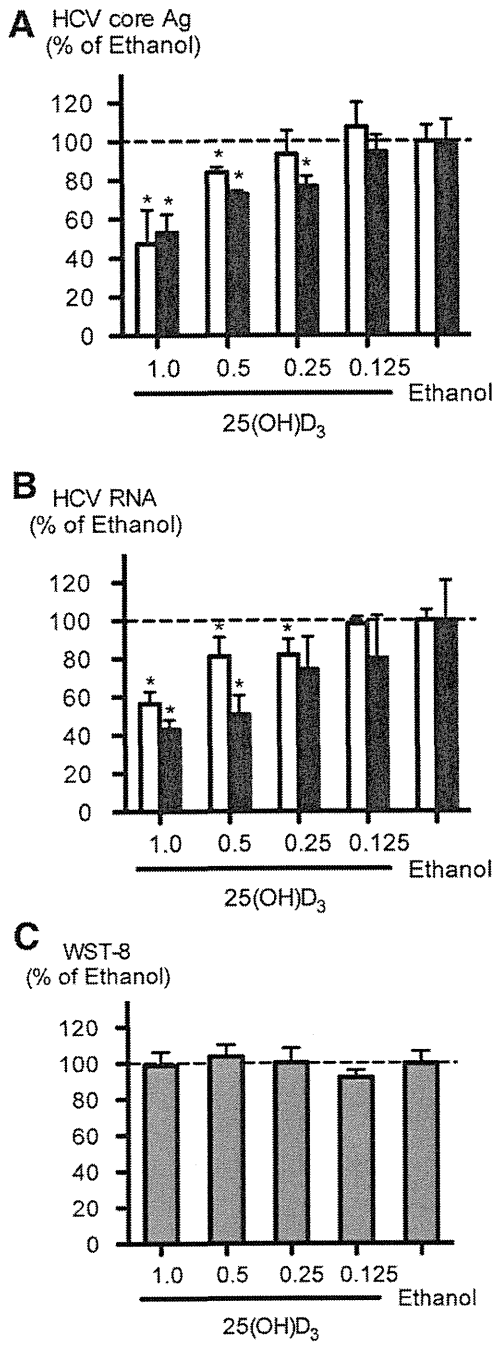

Fig. 2. Dose-dependent anti-HCV effects of $25(OH)D_3$. HuH-7 cells were treated with various concentrations of $25(OH)D_3$ followed by inoculation with HCVcc. HCV production was assessed by measuring the HCV core Ag. (A, B) HCV core Ag (A) and HCV RNA (B) in culture medium and cell lysates are indicated by white and black bars, respectively. $*P < 0.05$ versus ethanol. (C) Cell viability was assessed via WST-8 assay. Results are expressed as the mean ± SD of the percent of the control.

to 2 μM, and the calculated 50% cytotoxic concentration (CC_{50}) was 7.5 μM (Fig. 2C and Supporting Fig. 1B).

Effects of 25(OH)D$_3$ in HCV Life Cycle. To evaluate the effects of $25(OH)D_3$ on the HCV entry step, Huh-7.5.1 cells were infected with HCVpp harboring envelope glycoproteins of various HCV clones (H77, TH, JFH-1, and J6CF) or vesicular stomatitis virus in the presence of $25(OH)D_3$ (1.0, 0.5, and 0.25 μM), or ethanol. Treatment with $25(OH)D_3$ has no effects on the relative luciferase activity in the cells infected with HCVpp of any clone, suggesting that $25(OH)D_3$ does not affect the HCV entry (Fig. 3A).

To assess the effects of $25(OH)D_3$ on HCV replication, we used the HCV subgenomic replicon system. The reporter subgenomic replicon RNA containing luciferase reporter gene was transfected into HuH-7 cells, and the cells were treated with $25(OH)D_3$ at a concentration of 0.125 - 1.0 μM or with ethanol. Relative luciferase activities of $25(OH)D_3$-treated cells were comparable to those of ethanol-treated cells, indicating no effect on HCV replication (Fig. 3B).

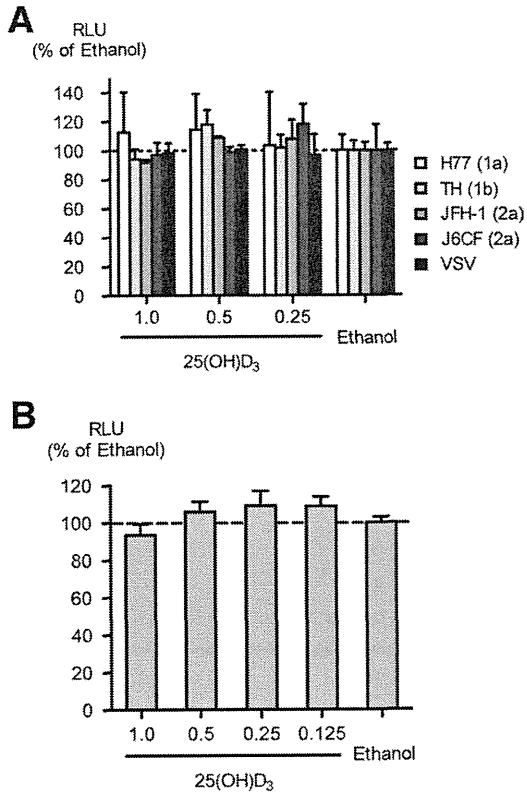

Fig. 3. Effect of $25(OH)D_3$ on HCV entry and replication. (A) HCVpp harboring E1 and E2 glycoproteins of various HCV clones and vesicular stomatitis virus G envelope glycoprotein were used to determine the effect of $25(OH)D_3$ on the entry step of HCV. Efficiency of HCVpp infection was estimated by measuring the luciferase activity. Results are expressed as the mean ± SD of the percent of the control. (B) HuH-7 cells were transfected with the subgenomic replicon RNAs and treated with various concentrations of $25(OH)D_3$. Replication efficiency of the replicon was estimated by measuring the luciferase activity. Results are expressed as the mean ± SD of the percentage of ethanol.

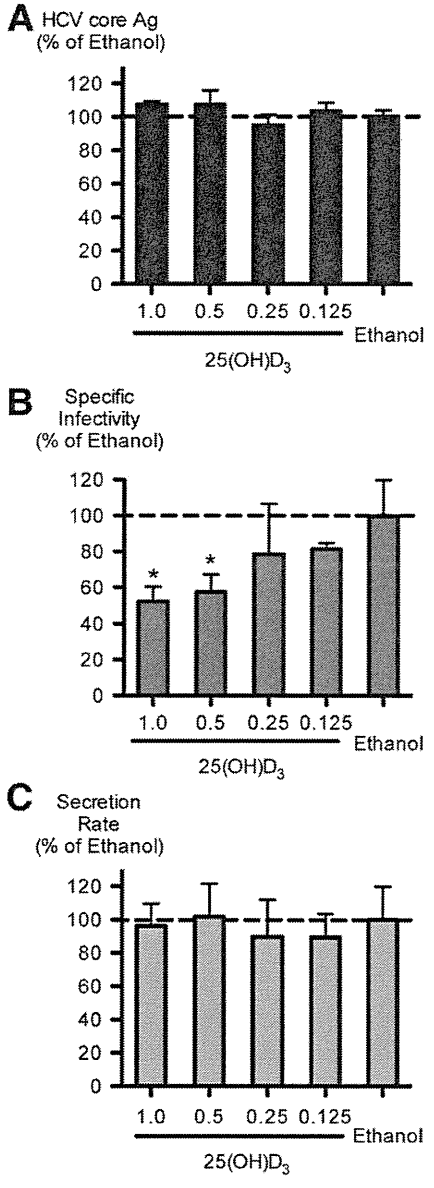

Fig. 4. Effects of 25(OH)D_3 on single-cycle virus production assay. Huh7-25 cells were transfected with JFH-1/wt RNA and treated with various concentrations of 25(OH)D_3. Intracellular HCV core Ag (A), intracellular specific infectivity (B), and the ratio of intra- to extracellular infectivity (secretion rate) (C) were determined. Results are expressed as the mean ± SD. *$P < 0.05$ versus ethanol.

Effects of 25(OH)D_3 in Single-Cycle Virus Production Assay. To further assess whether 25(OH)D_3 affects other steps of the viral life cycle, we used a single-cycle virus production assay with Huh7-25 cells lacking CD81 expression on the cell surface.[14] This cell line can support only replication and infectious virus production upon transfection of HCV genomic RNA but cannot be reinfected by produced HCV, therefore allowing the assessment of a single cycle of infectious viral production.[23] After a 3-day treatment with various concentrations of 25(OH)D_3, extra- and intracellular infectivity and intracellular HCV core Ag were determined. The intracellular levels of HCV core Ag in 25(OH)D_3-treated cells were similar to those of ethanol-treated cells (Fig. 4A and Supporting Table 1), corroborating the observation from the subgenomic replicon experiment. To estimate the efficiency of viral particle assembly, we next determined the intracellular specific infectivity by calculating the ratio of the intracellular infectivity titer over the intracellular HCV core Ag level. Indeed, 25(OH)D_3 at 0.5 and 1.0 μM reduced the intracellular-specific infectivity by approximately half compared with the control ($P < 0.05$) (Fig. 4B and Supporting Table 1). To estimate the infectious virus secretion, we determined the secretion rate by calculating the ratio of the extra- to intracellular infectivity. This analysis revealed no effects of 5(OH)D_3 on the secretion rate at any dose (Fig. 4C and Supporting Table 1).

Enhancement of Anti-HCV Effects of IFN by Supplementation of 25(OH)D_3. Vitamin D supplementation has been shown to improve the efficacy of IFN-based therapy. Therefore, we evaluated the anti-HCV effect of IFN-alpha2b via supplementation of 25(OH)D_3. HuH-7 cells were treated with IFN-alpha2b at concentrations of 1 or 10 IU/mL in combination with 25(OH)D_3 (1.0 μM) or ethanol and were infected with HCVcc. Treatment with 1 IU/mL of IFN-alpha2b reduced HCV core Ag levels in culture medium and cell lysate to 68.66 ± 2.17% and 41.18 ± 1.52% of the control, respectively (Fig. 5). Concomitant treatment with 25(OH)D_3 augments IFN-induced reduction in HCV core Ag levels by approximately two-fold. Similar effects of 25(OH)D_3 are observed with 10 IU/mL IFN-alpha2b.

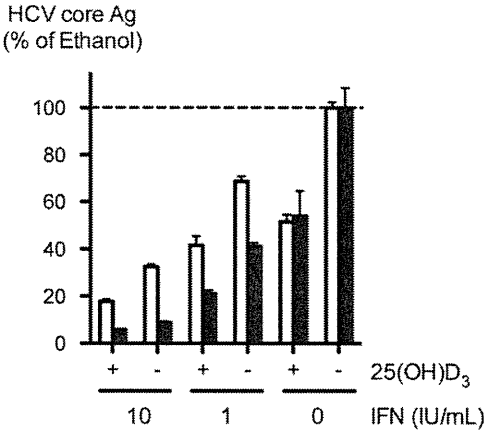

Fig. 5. Enhancement of anti-HCV effects of IFN via supplementation of 25(OH)D_3. HuH-7 cells were treated with IFN at the indicated concentrations in combination with 25(OH)D_3 (1.0 μM) or ethanol, followed by inoculation with HCVcc. HCV production was assessed by measuring the HCV core Ag. HCV core Ag levels in culture medium and cell lysates are indicated by white and black bars, respectively.

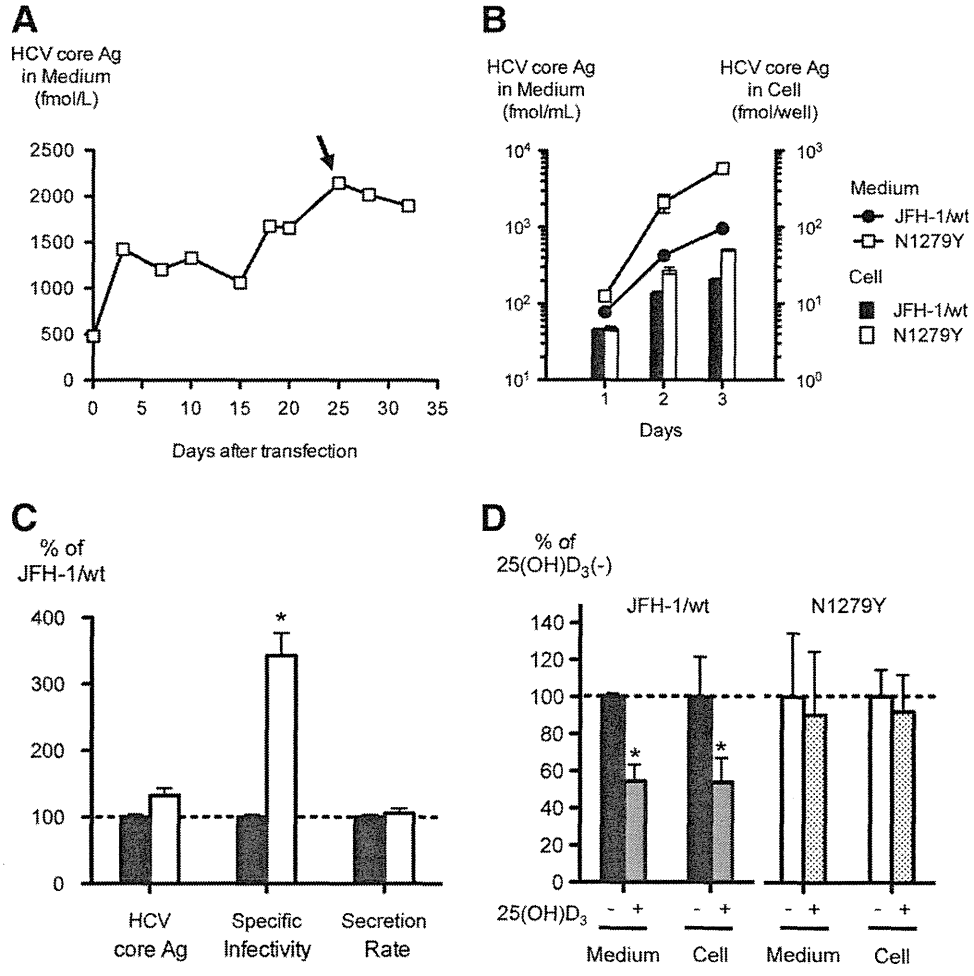

Fig. 6. Emergence of a resistant mutant in long-term culture with $25(OH)D_3$. (A) JFH-1/wt-transfected HuH-7 cells were continuously treated with $25(OH)D_3$ for 32 days to demonstrate the emergence of a resistant mutant. The level of HCV core Ag in culture medium was monitored. The peak point is indicated by an arrow. (B) Comparison of viral production between JFH-1/wt and N1279Y. HCV core Ag in culture medium (lines) and cell lysates (bars) were indicated. Results are expressed as the mean ± SD. (C) Single-cycle virus production assay with JFH-1 and N1279Y. Intracellular HCV core Ag, intracellular specific infectivity, and secretion rate of JFH-1/wt (black bars) and N1279Y (white bars) were depicted. Results are expressed as the mean ± SD of the percentage of JFH-1/wt. $*P < 0.05$ in comparison between N1279Y and wild-type. (D) Anti-HCV effects of $25(OH)D_3$ on JFH-1/wt and N1279Y. Infectivity titer in culture medium and cell lysates were determined. Results are expressed as the mean ± SD of the percentage of ethanol. $*P < 0.05$ versus ethanol.

Effects of 25(OH)D_3 on IFN-Stimulated Gene Induction. Vitamin D has emerged as a key regulator of innate immunity in humans. Type 1 IFN induces many effector molecules known as IFN-stimulated genes (ISGs) with antiviral activities. In order to assess the effects of $25(OH)D_3$ on ISG induction, HuH-7 cells were treated with IFN-alfa2b (10 IU/mL) in the presence or absence of $25(OH)D_3$ (1.0 μM), and the expression of MxA and 2′,5′-oligoadenylate synthetase messenger RNAs were determined by quantitative real-time PCR. The treatment with $25(OH)D_3$ does not affect either basal expression or IFN-mediated induction of MxA and 2′,5′-oligoadenylate synthetase (Supporting Fig. 2).

Isolation of 25(OH)D_3 Resistant Mutant. Next, we determined whether a long-term treatment with $25(OH)D_3$ leads to generation of a $25(OH)D_3$-resistant mutant in JFH-1 transfected cells. During a continuous treatment with $25(OH)D_3$ (1.0 μM) over a period of 32 days, the level of HCV core Ag in culture medium indeed increases gradually (Fig. 6A), suggesting an emergence of a mutant. Therefore, we harvested the culture medium at peak point at day 25, isolated the HCV RNA from the medium, and determined the sequence of entire ORF. Comparative sequencing of the JFH-1 has detected only one amino acid substitution of N to Y at amino acid 1279 (N1279Y) in nonstructural region 3 (NS3). To test the characteristics of this amino acid substitution, we generated a full-genome JFH-1 construct with this substitution (N1279Y) and compared virus replication and production with the wild-type JFH-1 (JFH-1/wt). After transfection of RNA of JFH-1/wt or N1279Y into Huh-7.5.1 cells, HCV core Ag in culture medium and cell lysate were quantified. Both intra- and extracellular levels of HCV core Ag from the N1279Y-transfected cells were significantly higher than those of JFH-1/wt transfected cells ($P < 0.05$) (Fig. 6B). To analyze the effects of this substitution on different stages of the virus life cycle, we performed a single-cycle virus production assay. We compared intracellular HCV core Ag, intracellular specific infectivity, and secretion rate via transfection of JFH-1/wt and N1279Y RNAs into Huh7-25 cells. Our results show that the intracellular specific infectivity was 3.4-fold higher in N1279Y-transfected cells than in JFH-1/wt–transfected cells.

On the other hand, the intracellular core Ag level and secretion rate were not affected by this substitution (Fig. 6C and Supporting Table 2). To test whether this amino acid substitution confers the resistance to the inhibitory effect of $25(OH)D_3$, we compared the effect on infectious virus production. As predicted, treatment with $25(OH)D_3$ at a concentration of 1.0 μM reduced intra- and extracellular infectivity titer in JFH-1/wt–transfected cells to 54.5 ± 9.0 and 59.1 ± 14.4% of the control, respectively ($P < 0.05$). However, in N1279Y-transfected cells, these effects were completely abrogated (Fig. 6D), suggesting that the N1279Y mutation was responsible for the $25(OH)D_3$ resistance.

Anti-HCV Effects of $25(OH)D_3$ in Multiple HCV Strains Other than JFH-1. To assess the strain specificity, we also examined the anti-HCV effect of $25(OH)D_3$ using other HCV strains, J6/JFH-1, H77S.2, and JFH-1 with V2440L mutation (JFH-1/V2440L). Treatment with $25(OH)D_3$ reduced intra- and extracellular infectivity titers of these strains to 25.2-48.2% of the ethanol control (Supporting Fig. 3). Thus, these strains are also susceptible to $25(OH)D_3$.

Production of $1,25(OH)_2D_3$ in Cell Culture. Finally, we tested the possibility that the anti-HCV effect of $25(OH)D_3$ is mediated by $1,25(OH)_2D_3$ generated from $25(OH)D_3$ in the cells. HuH-7 cells were treated with $25(OH)D_3$ at various concentrations, and production of $1,25(OH)_2D_3$ was measured. After treatment of $25(OH)D_3$ at 5.0 and 2.0 μM, the concentrations of $1,25(OH)_2D_3$ detected in the culture medium were 365.62 ± 30.01 and 104.49 ± 11.08 pM, respectively, and are slightly higher than that with ethanol treatment (Supporting Fig. 4A). After treatment of $25(OH)D_3$ at 1.0 and 0.5 μM, the $1,25(OH)_2D_3$ concentrations are similar to that of ethanol treatment. We then evaluated whether the concentrations of $1,25(OH)_2D_3$ ranging from 0.01 to 1.0 μM have an anti-HCV effect on HCVcc-infected cells. This study revealed no anti-HCV effect at any concentration studied, although an anti-HCV effect of $25(OH)D_3$ is reproducible (Supporting Fig. 4B).

Discussion

Vitamin D is reported to have regulatory roles in infectious diseases[12,24] and to act as an immune modulator in both innate and adaptive immune pathways.[25,26] In patients with chronic hepatitis C, low serum levels of vitamin D are associated with severe fibrosis, and poor responsiveness to IFN-based therapy has been reported.[27] Furthermore, vitamin D supplementation significantly improves the SVR rate of combination IFN and ribavirin therapy in patients with hepatitis C.[5,6] These studies postulated that $1,25(OH)_2D$, the active metabolite of 25(OH)D, is responsible for the effects. However, our current study using the culture model, identifies $25(OH)D_3$ but not $1,25(OH)_2D_3$ as an effective anti-HCV metabolite with the ability to suppress infectious virus production (Figs. 1 and 2). By using HCVpp and a subgenomic replicon system, we found that $25(OH)D_3$ did not influence the steps of HCV entry and replication (Fig. 3) but rather selectively inhibited the virus assembly step (Fig. 4). We believe that this finding offers a novel mechanistic insight into the therapeutic efficacy of supplemental vitamin D observed in HCV patients.

Detailed mechanisms of the anti-HCV effect of $25(OH)D_3$ are still elusive. The biological activity of vitamin D is mainly attributed to $1,25(OH)_2D$, the most active form of vitamin D, and 25(OH)D has only been regarded as a pro-hormone with no ascribed direct biological functions. However, a recent study demonstrates gene regulatory effects of $25(OH)D_3$ in a manner dependent on vitamin D receptor and its synergism with $1,25(OH)_2D_3$.[28] It is still unclear whether 25(OH)D has direct targets or biological functions different from those of $1,25(OH)_2D$. Our study demonstrates in HCVcc-infected cells a clear difference in the effect on HCV viral assembly rendered by $25(OH)D_3$ versus $1,25(OH)_2D_3$, with only the former having an inhibitory effect (Fig. 1, Supporting Fig. 4); this finding suggests that the common signaling pathway cannot underlie this discrete action. The treatment with $25(OH)D_3$ may induce specific host factors involved in inhibition of infectious HCV production. To this end, we evaluated ISG induction by $25(OH)D_3$ with or without IFN treatment, but no effects were observed (Supporting Fig. 2), suggesting that involvement of ISGs is unlikely in the observed effect of $25(OH)D_3$.

The anti-HCV effect of $25(OH)D_3$ is limited in its potency; infectious virus production is reduced only to half of controls (Figs. 1 and 2). This reduction may not be sufficient when it is used as a sole anti-HCV agent. Moreover, in our long-term culture experiment with $25(OH)D_3$, the JFH-1–resistant mutant emerged (Fig. 6). We cloned and sequenced this mutant to demonstrate that the N1279Y substitution in NS3 is responsible for the resistance (Fig. 6D), although this amino acid polymorphism is not observed among deposited strains in the Hepatitis Virus Database (http://s2as02.genes.nig.ac.jp/). NS3 is known to code

protease and helicase, and the detected substitution is in the helicase domain. This substitution is associated with a marked enhancement of assembly efficiency of infectious virus particles (Fig. 6C). As the involvement of the NS3 helicase domain in virion morphogenesis is reported,[29] the observed suppressive effect of 25(OH)D_3 may be associated with this specific function of NS3. Collectively, our findings suggest that the treatment of hepatitis C with 25(OH)D_3 alone may not be recommended because of a limited antiviral effect and emergence of the resistant mutant. However, if it is combined with compounds that inhibit the HCV replication such as IFN or protease inhibitors, it should optimize the antiviral effect while minimizing the genesis of the mutant. Indeed, we confirm the enhancement of anti-HCV effect of IFN by supplementation of 25(OH)D_3 (Fig. 5).

The effective concentrations of 25(OH)D_3 shown in our study may seem too high. We used 1 μM of 25(OH)D_3 to observe the sufficient reduction of infectious virus production (Fig. 2). This concentration is almost 10-fold higher than the peripheral concentration in normal subjects. However, the actual concentration of 25(OH)D may be much higher in the liver where this metabolite is primarily produced. Because HCV replicates in the same hepatocellular site, 25(OH)D may be sufficiently concentrated to render an immediate anti-HCV effect. On the other hand, low 25(OH)D levels are reported in patients with cirrhosis or severe hepatic dysfunction.[30-33] A depressed activity of 25-hydroxylase in damaged livers in these patients may be responsible for this observation. Therefore, 25(OH)D, not vitamin D, should be a better antiviral agent in such patients as a supplement for IFN and ribavirin therapy.

In a recent report, Gal-Tanamy et al.[34] describe the anti-HCV effects of vitamin D. In this study, treatment with vitamin D_3 or 1,25$(OH)_2D_3$ reduced infectious virus production by Huh-7.5 cells infected with HCV H77-JFH-1 intergenotypic chimeric virus. The effects are ascribed to enhancement of IFN-beta expression and ISG induction by 1,25(OH)2D_3. In our experiments, we did not observe such anti-HCV effects of vitamin D_3 or 1,25$(OH)_2D_3$ at the concentrations similar to those used by Gal-Tanamy et al. This discrepancy might be related to the different systems used for analyses. The anti-HCV activities of vitamin D and its metabolites may be different among HCV strains and cell lines. Further studies will be needed to resolve this discrepancy.

In conclusion, 25(OH)D_3 is identified as a novel anti-HCV agent that selectively targets the infectious viral particle assembly step. This observation provides the basis for the improvement of efficacy of anti-HCV treatment by supplementation of vitamin D to IFN and ribavirin therapy. Our study also provides the possibility that the supplementation of 25(OH)D would be indicated in patients with compromised hepatic functions. Clinical studies are required to evaluate a possible therapeutic use of 25(OH)D.

Acknowledgment: We are grateful to Francis V. Chisari (Scripps Research Institute, La Jolla, CA) for Huh-7.5.1 cells and to Stanley M. Lemon (University of North Carolina at Chapel Hill, Chapel Hill, NC) for pH77S.2 the plasmid for H77S.2 (replication competent genotype 1a strain).

References

1. Liang TJ, Rehermann B, Seeff LB, Hoofnagle JH. Pathogenesis, natural history, treatment, and prevention of hepatitis C. Ann Intern Med 2000;132:296-305.
2. Seeff LB, Hoofnagle JH. National Institutes of Health Consensus Development Conference: management of hepatitis C: 2002. HEPATOLOGY 2002;36:S1-S2.
3. Feld JJ, Hoofnagle JH. Mechanism of action of interferon and ribavirin in treatment of hepatitis C. Nature 2005;436:967-972.
4. Pawlotsky JM. Therapy of hepatitis C: from empiricism to eradication. HEPATOLOGY 2006;43:S207-S220.
5. Bitetto D, Fabris C, Fornasiere E, Pipan C, Fumolo E, Cussigh A, et al. Vitamin D supplementation improves response to antiviral treatment for recurrent hepatitis C. Transpl Int 2011;24:43-50.
6. Abu-Mouch S, Fireman Z, Jarchovsky J, Zeina AR, Assy N. Vitamin D supplementation improves sustained virologic response in chronic hepatitis C (genotype 1)-naive patients. World J Gastroenterol 2011; 17:5184-5190.
7. Imawari M, Kida K, Goodman DS. The transport of vitamin D and its 25-hydroxy metabolite in human plasma. Isolation and partial characterization of vitamin D and 25-hydroxyvitamin D binding protein. J Clin Invest 1976;58:514-523.
8. Garland CF, Garland FC, Gorham ED, Lipkin M, Newmark H, Mohr SB, et al. The role of vitamin D in cancer prevention. Am J Public Health 2006;96:252-261.
9. VanAmerongen BM, Dijkstra CD, Lips P, Polman CH. Multiple sclerosis and vitamin D: an update. Eur J Clin Nutr 2004;58:1095-1109.
10. Zittermann A. Vitamin D and disease prevention with special reference to cardiovascular disease. Prog Biophys Mol Biol 2006;92:39-48.
11. Davies PD, Brown RC, Woodhead JS. Serum concentrations of vitamin D metabolites in untreated tuberculosis. Thorax 1985;40:187-190.
12. Muhe L, Lulseged S, Mason KE, Simoes EA. Case-control study of the role of nutritional rickets in the risk of developing pneumonia in Ethiopian children. Lancet 1997;349:1801-1804.
13. Chiu KC, Chu A, Go VLW, Saad MF. Hypovitaminosis D is associated with insulin resistance and β cell dysfunction. Am J Clin Nutr 2004; 79:820-825.
14. Akazawa D, Date T, Morikawa K, Murayama A, Miyamoto M, Kaga M, et al. CD81 expression is important for the permissiveness of Huh7 cell clones for heterogeneous hepatitis C virus infection. J Virol 2007; 81:5036-5045.
15. Wakita T, Pietschmann T, Kato T, Date T, Miyamoto M, Zhao Z, et al. Production of infectious hepatitis C virus in tissue culture from a cloned viral genome. Nat Med 2005;11:791-796.

16. Takeuchi T, Katsume A, Tanaka T, Abe A, Inoue K, Tsukiyama-Kohara K, et al. Real-time detection system for quantification of hepatitis C virus genome. Gastroenterology 1999;116:636-642.
17. Aoyagi K, Ohue C, Iida K, Kimura T, Tanaka E, Kiyosawa K, et al. Development of a simple and highly sensitive enzyme immunoassay for hepatitis C virus core antigen. J Clin Microbiol 1999;37:1802-1808.
18. Ishiyama M, Miyazono Y, Sasamoto K, Ohkura Y, Ueno K. A highly water-soluble disulfonated tetrazolium salt as a chromogenic indicator for NADH as well as cell viability. Talanta 1997;44:1299-1305.
19. Bartosch B, Dubuisson J, Cosset FL. Infectious hepatitis C virus pseudo-particles containing functional E1-E2 envelope protein complexes. J Exp Med 2003;197:633-642.
20. Bartosch B, Vitelli A, Granier C, Goujon C, Dubuisson J, Pascale S, et al. Cell entry of hepatitis C virus requires a set of co-receptors that include the CD81 tetraspanin and the SR-B1 scavenger receptor. J Biol Chem 2003;278:41624-41630.
21. Kato T, Date T, Miyamoto M, Sugiyama M, Tanaka Y, Orito E, et al. Detection of anti-hepatitis C virus effects of interferon and ribavirin by a sensitive replicon system. J Clin Microbiol 2005;43:5679-5684.
22. Kato T, Date T, Murayama A, Morikawa K, Akazawa D, Wakita T. Cell culture and infection system for hepatitis C virus. Nat Protoc 2006;1:2334-2339.
23. Kato T, Choi Y, Elmowalid G, Sapp RK, Barth H, Furusaka A, et al. Hepatitis C virus JFH-1 strain infection in chimpanzees is associated with low pathogenicity and emergence of an adaptive mutation. HEPATOLOGY 2008;48:732-740.
24. Yuk JM, Shin DM, Lee HM, Yang CS, Jin HS, Kim KK, et al. Vitamin D3 induces autophagy in human monocytes/macrophages via cathelicidin. Cell Host Microbe 2009;6:231-243.
25. Lin R, White JH. The pleiotropic actions of vitamin D. Bioessays 2004;26:21-28.
26. Liu PT, Modlin RL. Human macrophage host defense against Mycobacterium tuberculosis. Curr Opin Immunol 2008;20:371-376.
27. Petta S, Camma C, Scazzone C, Tripodo C, Di Marco V, Bono A, et al. Low vitamin D serum level is related to severe fibrosis and low responsiveness to interferon-based therapy in genotype 1 chronic hepatitis C. HEPATOLOGY 2010;51:1158-1167.
28. Lou YR, Molnar F, Perakyla M, Qiao S, Kalueff AV, St-Arnaud R, et al. 25-Hydroxyvitamin D(3) is an agonistic vitamin D receptor ligand. J Steroid Biochem Mol Biol 2010;118:162-170.
29. Jones DM, Atoom AM, Zhang X, Kottilil S, Russell RS. A genetic interaction between the core and NS3 proteins of hepatitis C virus is essential for production of infectious virus. J Virol 2011;85:12351-12361.
30. Monegal A, Navasa M, Guanabens N, Peris P, Pons F, Martinez de Osaba MJ, et al. Osteoporosis and bone mineral metabolism disorders in cirrhotic patients referred for orthotopic liver transplantation. Calcif Tissue Int 1997;60:148-154.
31. Hofmann WP, Kronenberger B, Bojunga J, Stamm B, Herrmann E, Bucker A, et al. Prospective study of bone mineral density and metabolism in patients with chronic hepatitis C during pegylated interferon alpha and ribavirin therapy. J Viral Hepat 2008;15:790-796.
32. Imawari M, Akanuma Y, Itakura H, Muto Y, Kosaka K, Goodman DS. The effects of diseases of the liver on serum 25-hydroxyvitamin D and on the serum binding protein for vitamin D and its metabolites. J Lab Clin Med 1979;93:171-180.
33. Masuda S, Okano T, Osawa K, Shinjo M, Suematsu T, Kobayashi T. Concentrations of vitamin D-binding protein and vitamin D metabolites in plasma of patients with liver cirrhosis. J Nutr Sci Vitaminol (Tokyo) 1989;35:225-234.
34. Gal-Tanamy M, Bachmetov L, Ravid A, Koren R, Erman A, Tur-Kaspa R, et al. Vitamin-D: an innate antiviral agent suppressing Hepatitis C virus in human hepatocytes. HEPATOLOGY 2011;54:1570-1579.

JVI
Journals.ASM.org

Novel Cell Culture-Adapted Genotype 2a Hepatitis C Virus Infectious Clone

Tomoko Date,[a] Takanobu Kato,[a] Junko Kato,[b] Hitoshi Takahashi,[a]* Kenichi Morikawa,[a,c]* Daisuke Akazawa,[a,d] Asako Murayama,[a] Keiko Tanaka-Kaneko,[e] Tetsutaro Sata,[e]* Yasuhito Tanaka,[f] Masashi Mizokami,[g] and Takaji Wakita[a]

Department of Virology II, National Institute of Infectious Diseases, Tokyo,[a] Institute of Geriatrics, Tokyo Women's Medical University, Tokyo,[b] Division of Gastroenterology, Department of Medicine, Showa University School of Medicine, Tokyo,[c] Pharmaceutical Research Laboratories, Toray Industries, Inc., Kanagawa,[d] Department of Pathology, National Institute of Infectious Diseases, Tokyo,[e] Department of Virology and Liver Unit, Nagoya City University Graduate School of Medical Sciences, Nagoya,[f] and The Research Center for Hepatitis and Immunology, National Center for Global Health and Medicine, Chiba,[g] Japan

Although the recently developed infectious hepatitis C virus system that uses the JFH-1 clone enables the study of whole HCV viral life cycles, limited particular HCV strains have been available with the system. In this study, we isolated another genotype 2a HCV cDNA, the JFH-2 strain, from a patient with fulminant hepatitis. JFH-2 subgenomic replicons were constructed. HuH-7 cells transfected with *in vitro* transcribed replicon RNAs were cultured with G418, and selected colonies were isolated and expanded. From sequencing analysis of the replicon genome, several mutations were found. Some of the mutations enhanced JFH-2 replication; the 2217AS mutation in the NS5A interferon sensitivity-determining region exhibited the strongest adaptive effect. Interestingly, a full-length chimeric or wild-type JFH-2 genome with the adaptive mutation could replicate in Huh-7.5.1 cells and produce infectious virus after extensive passages of the virus genome-replicating cells. Virus infection efficiency was sufficient for autonomous virus propagation in cultured cells. Additional mutations were identified in the infectious virus genome. Interestingly, full-length viral RNA synthesized from the cDNA clone with these adaptive mutations was infectious for cultured cells. This approach may be applicable for the establishment of new infectious HCV clones.

Hepatitis C virus (HCV) is a principal agent in posttransfusion and sporadic acute hepatitis (6, 19). HCV belongs to the *Flaviviridae* family and *Hepacivirus* genus. Infection with HCV leads to chronic liver diseases, including cirrhosis and hepatocellular carcinoma (16). HCV is a major public health problem, infecting an estimated 170 million people worldwide (6, 16, 19). Current standard therapy for HCV-related chronic hepatitis is based on the combination of interferon (IFN) and ribavirin although virus eradication rates are limited to around 50% (7, 24, 30). Telaprevir and boceprevir were approved by the U.S. Food and Drug Administration in 2011 in combination with pegylated alpha interferon and ribavirin for the treatment of genotype 1 chronic hepatitis C (34, 35). Both agents inhibit the NS3-NS4A serine protease essential for replication of HCV (25, 36). It is important to develop more anti-HCV drugs with different modes of action to achieve greater efficacy and to avoid the emergence of drug-resistant viruses. To that end, a detailed understanding of the viral replication mechanism is needed to discover novel antiviral targets. An efficient virus culture system is indispensable for detailed analysis of HCV life cycles. In an important development, a subgenomic HCV RNA replicon system has been developed (22) to assess HCV replication in cultured cells. Furthermore, an efficient HCV culture system was established by using a JFH-1 strain virus isolated from a fulminant hepatitis patient (20, 38, 41). By transfection of *in vitro* transcribed full-length JFH-1 HCV RNA into HuH-7 cells, efficient JFH-1 RNA replication and infectious viral particle production were detected. However, this efficient virus production was not reproduced by other HCV strains, even when adaptive mutations were introduced to enhance the replication efficiency in cultured cells (29). Thus, other HCV strains that can replicate in cultured cells and produce infectious virus particles are needed. The J6CF strain is infectious to chimpanzees but does not replicate in cultured cells (26, 27, 40). We constructed chimeric replicon and virus constructs of the J6CF and JFH-1 strains to elucidate the difference in their molecular mechanisms (26, 27). We determined that the NS3 helicase and the NS5B to 3′X regions are important for the efficient replication of the JFH-1 strain and that several amino acid mutations in the C terminus of NS5B are pivotal for replication. However, we could not rescue the replication of other virus strains, such as Con1, with these mutations. This result indicates that different approaches are needed to create replication-competent virus strains in cultured cells.

In the present study, we isolated HCV cDNA, named JFH-2, from a fulminant hepatitis patient. The replication efficiency of the JFH-2 clone in the subgenomic replicon assay was lower than that of JFH-1 although the introduction of adaptive mutations enhanced JFH-2 replication. Interestingly, the full-length chimeric or wild-type JFH-2 genome with adaptive mutations could replicate and produce infectious virus particles. The virus infection efficiency was sufficient for autonomous virus propagation in cultured cells.

MATERIALS AND METHODS

Cell culture system. HuH-7, Huh-7.5.1 (a generous gift from Francis V. Chisari), and Huh7-25 cells were cultured in 5% CO_2 at 37°C in Dulbec-

Received 29 December 2011 Accepted 2 July 2012
Published ahead of print 11 July 2012
Address correspondence to Takaji Wakita, wakita@nih.go.jp.
* Present address: Hitoshi Takahashi, Influenza Virus Research Center, National Institute of Infectious Diseases, Musashimurayama, Tokyo, Japan; Kenichi Morikawa, Division of Gastroenterology and Hepatology, Centre Hospitalier Universitaire Vaudois, University of Lausanne, Lausanne, Switzerland; Tetsutaro Sata, Toyama Institute of Health, Toyama, Japan.

doi:10.1128/JVI.07235-11

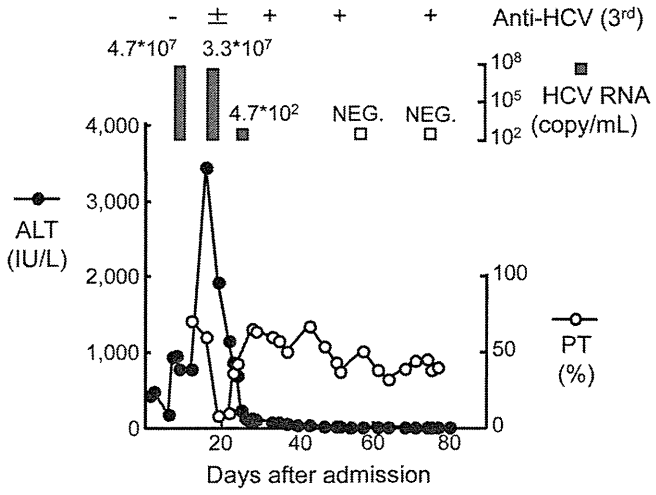

FIG 1 Clinical course of second fulminant hepatitis patient infected with JFH-2. The patient was admitted by reason of acute liver failure. Alanine aminotransferase (ALT) levels, prothrombin time (PT), HCV RNA, and anti-HCV antibodies were determined and followed in his serum.

co's modified Eagle's medium (DMEM) containing 10% fetal bovine serum (DMEM-10) (3, 41).

HCV clones. The genotype 2a clone JFH-2 was isolated from a patient with fulminant hepatitis (15). Briefly, HCV cDNA was cloned from a fulminant hepatitis patient, a 62-year-old man who had a history of coronary artery bypass surgery without blood transfusion. One year after the surgery, he developed an acute auditory disorder and received a course of betamethasone therapy. After withdrawal of betamethasone, the patient developed fulminant hepatitis as diagnosed by acute liver failure associated with stage II encephalopathy and low prothrombin time. He experienced prolonged liver failure and died after 80 days. HCV RNA was detected in his serum only during the acute phase (Fig. 1). Total RNA was extracted from serum during the acute phase, and HCV cDNA covering the entire genome was amplified by reverse transcription-PCR (RT-PCR). All amplified products were purified and then cloned into pGEM-T EASY vectors (Promega, Madison, WI). PCR products and plasmids were sequenced by using specific primer sets (Table 1), BigDye Terminator Mix, and an automated DNA sequencer (models 310 and 377; PE Biosystems, Foster City, CA). The JFH-2 subgenomic replicon (SGR) clones, pSGR-JFH2.1 and pSGR-JFH2.2 (DDBJ/EMBL/GenBank accession numbers AB690456 and AB690457, respectively), were constructed according to the method for pSGR-JFH1 construction (11). Several mutations were introduced into the pSGR-JFH2.1 replicon construct, as reported previously (11). The reporter replicon constructs, pSGR-JFH2.1/Luc and pSGR-JFH2.1/Luc, were developed by rearrangement with pSGR-JFH2.1 and pSGR-JFH2.2 (accession numbers AB690458 and AB690459, respectively) as described previously (12). pJ6/JFH1 was previously obtained from pJFH1 by replacement with the 5′ untranslated region (UTR) to the p7 region (EcoRI-BclI) of the J6CF strain (a kind gift from Jens Bukh) (3, 40). A full-length HCV cDNA was constructed by using the 5′ end to NS2 of pJ6/JFH1 and NS3 to the 3′ end of pSGR-JFH2.1, and the resulting construct was named pJ6/JFH2 (accession number AB690460). Another full-length HCV construct, pJFH2 containing the full-length JFH-2 cDNA downstream of the T7 RNA promoter sequence, was also constructed by replacing the 5′ UTR to NS2 of pJ6/JFH2 with JFH2 sequences, as described previously (accession number AB690461) (1, 37, 38).

Subgenomic replicon assay. Subgenomic replicon RNA was synthesized as reported previously (11). Synthesized replicon RNA was adjusted to 10 μg with cellular RNA isolated from untransfected HuH-7 cells and then electroporated into naive HuH-7 cells as reported previously (11). G418 (1.0 mg/ml) was added to the culture medium, and the drug-resistant colonies were fixed with buffered formalin and stained with crystal violet or cloned and expanded for further analysis. Total RNA was extracted from the cloned G418-resistant cells by using Isogen reagent (Nip-

TABLE 1 Primer list used for cloning and sequencing of JFH-2 clone

Forward primer		Reverse primer	
Name	Sequence (5′→3′)	Name	Sequence (5′→3′)
44S	CTGTGAGGAACTACTGTCTT	1323R	GGTGACCAGTTCATCATCAT
317S	GGGAGGTCTCGTAGACCGTG	1440R	GCTCCCTGCATAGAGAAGTA
844S	GGGTTAATTATGCAACAGGGAAC	2367R	CATTCCGTGGTAGAGTGCA
1141S	TGTCCGCCACGCTCTGCT	2445R	TCCACGATGTTTTGGTGGAG
1361S	CCCGAGGTCATCATAGACAT	3568R	TGTTCCGAGGAAGGACTGAG
2106S	CTGTTGTGCCCCACGGACTG	3765R	TCAGCGTTCCGCGTGACCA
2285S	AACTTCACTCGTGGGGATCG	4706R	TTGCAGTCGATCACGGAGTC
3211S	GGCACTTACATCTATGACCACCTC	5331R	GAGGTCATGACCAGCACGTG
3471S	TGGGCACCATAGTGGTGAG	5563R	CTGCAGCAAGCCTTGGATCT
3930S	TCGATTTCATCCCCGTTGAG	5970R	TTCTCGCCAGACATGATCTT
4278S	CCTATGACATCATCATATGCGATGAATGCC	6152R	AGTGAGTAGGGGCGACGTGGTTTCCTCTGG
4301S	CCTATGACATCATCATATGCGATG	6505R	CCTGCCAGGTGTTCATGCAG
4547S	AAGTGTGACGAGCTCGCGG	6605R	GCATACTCTGAGGCCGCCAC
5021S	TTTTGGGAGGCAGTTTTCAC	6897R	GTGATGTGGGGCGGATCTGTTAGCATGGAC
6383S	TGTCAAAAGGGGTACAAGGG	7648R	TCCTCCTCGGAGCAAGTAGA
6774S	TCCGGGATGAGGTCTCGTTC	8913R	GCGTACTGGATGATGTTTCC
6881S	ATTGATGTCCATGCTAACAG	3X-54R	GCGGCTCACGGACCTTTCAC
7198S	GGCTTGGGCACGGCCTGA	3X-75R	TACGGCACTCTCTGCAGTCA
7244S	ACCGCTTGTGGAATCGTGGA		
7657S	CGTGTGCTGCTCCATGTCAT		
7993S	CAGCTTGTCCGGGAGGGC		
8337S	TTTCGTATGATACCCGATGCTT		
8704S	CGCCCCTCCGGGTGACCCCCCCAGACCGGA		
9123S	CACGAACTGACGCGGGTGGC		

pon Gene, Tokyo, Japan), and the replicon RNA was quantitated by Northern blotting and real-time detection RT-PCR as reported previously (11, 37). The cDNAs of the HCV RNA replicon were synthesized and then amplified by PCR. The sequence of each replicon was determined.

Luciferase reporter replicons were analyzed as follows. Five micrograms of synthesized replicon RNA was transfected into HuH-7 cells by electroporation. Transfected cells were harvested serially at 4, 24, 48, 72, and 96 h after transfection. Luciferase activities were quantified by a Lumat LB9507 instrument (EG&G Berthold, Bad Wildbad, Germany) and a luciferase assay system (Promega). Assays were performed at least in triplicate, and the results were expressed as relative luciferase activity.

Analysis of G418-resistant cells. In RNA-transfected dishes, G418-resistant colonies were isolated by using a cloning cylinder (Asahi Techno Glass Co., Tokyo, Japan) and expanded until 80% to 90% confluence in 10-cm diameter dishes. Expanded cells were analyzed as described previously (11).

Northern blot analysis. Four micrograms of isolated RNA samples was electrophoretically separated in a 1% agarose gel containing formaldehyde and transferred to a positively charged nylon membrane (Hybond-N+; GE Healthcare UK, Ltd., Buckinghamshire, England) and immobilized by a Stratalinker UV cross-linker (Stratagene, La Jolla, CA). Hybridization was performed with a [α-^{32}P]dCTP-labeled DNA probe by using Rapid-Hyb Buffer (GE Healthcare UK, Ltd.). The NS3 to 3′X region of the JFH-1 sequence was used as a template of DNA probe synthesis with a Megaprime DNA Labeling System (GE Healthcare UK, Ltd.) (37).

Western blot analysis of HCV proteins. The protein samples were separated on a 10% polyacrylamide gel. After electrophoresis, the proteins were transferred to a polyvinylidene difluoride membrane (Immobilon; Millipore Corp., Bedford, MA) with a semidry blotting apparatus (Biocraft, Tokyo, Japan). Transferred proteins were incubated with blocking buffer containing 5% nonfat dry milk (Snow brand, Sapporo, Japan) in phosphate-buffered saline. Anti-NS3 rabbit polyclonal antibody raised against recombinant NS3 protein and horseradish peroxidase-labeled goat anti-rabbit Ig (BioSource, Camarillo, CA) were used to detect HCV NS3 protein. The signals were detected with a chemiluminescence system (ECL Plus; GE Healthcare UK, Ltd.). The quantity and quality of the loaded samples were confirmed to be similar by Coomassie brilliant blue staining of the gel.

RT-PCR and sequencing analysis. The cDNAs of HCV RNA were synthesized from total cellular RNA isolated from replicon RNA-transfected cells or from the culture medium of full-length HCV RNA-transfected cells with antisense primer in the 3′X tail region. These cDNAs were subsequently amplified with DNA polymerase (TaKaRa LA Taq; TaKaRa Bio Inc.). The sequence of each amplified DNA was determined directly as described above.

Full-length HCV RNA transfection. Full-length HCV RNA was synthesized from pJ6/JFH2, pJFH2, and the derivatives of these constructs with adaptive mutations, as described previously (13, 37, 38). Synthesized HCV RNA (10 μg) was transfected into Huh-7.5.1 or Huh7-25 cells. HCV core protein levels in the culture medium were measured by immunoassay (31). HCV RNA levels in the culture medium were quantified as described above. Infectivity of culture supernatants was determined by measuring the focus formation efficiency (13, 41). In some experiments, HCV core protein levels in the transfected cells were determined as described previously (37, 38). To examine virus secretion and infectivity after long-term culture, the transfected cells were serially passaged. Virus infection was neutralized by using mouse anti-CD81 monoclonal antibody (clone JS-81; BD Pharmingen, Franklin Lakes, NJ) and anti-HCV human IgG purified from HCV carrier serum (a gift from H. Yoshizawa and J. Tanaka, Hiroshima University).

Density gradient analysis. Culture medium derived from the transfected or infected cells was harvested for density gradient analysis. Cleared culture medium was layered onto a stepwise sucrose gradient (60% [wt/vol] to 10%) and centrifuged for 16 h in an SW41 rotor (Beckman, Palo Alto, CA) at 200,000 $\times$ *g* at 4°C. After centrifugation, 18 fractions were harvested from the bottom of the tubes. The HCV core protein, HCV RNA levels, and infectivity in each fraction were determined as described above.

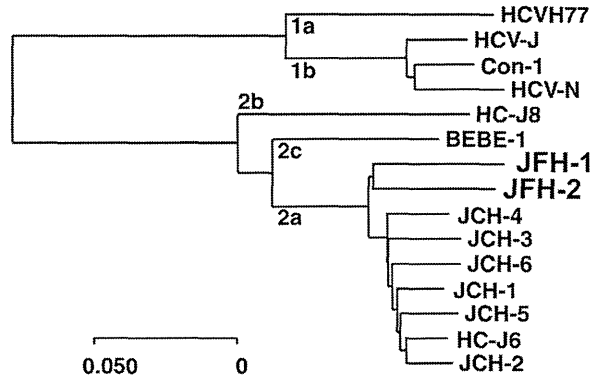

FIG 2 Phylogenetic analysis of JFH-2. Phylogenetic tree of the NS3 to NS5B amino acid sequences of HCV including the JFH-2 strain and genotype 2 strains for which the entire genome has been reported (JFH-1, accession number AB047639; HC-J6, D00944; HC-J8, D10988; and BEBE1, D50409) and representative genotype 1 strains for which the entire genome has been reported (H77, AF009606; HCV-Con1, AJ238799; HCV-J, D90208, and HCV-N, AF139594). This phylogenetic tree was drawn by using Kimura's two-parameter method.

Electron microscopy. To visualize HCV particles, we adsorbed the density gradient-purified virus samples onto carbon-coated grids for 1 min. Then, the grids were stained with 1% uranyl acetate for 1 min and examined under an H-7650 transmission electron microscope (Hitachi High-Technologies Co., Tokyo, Japan) (32). Immunogold labeling was performed with an antibody directed against E2 (AP33; a kind gift from Genentech, South San Francisco, CA) diluted 1:50 in blocking solution and secondary antibody coupled to 10-nm gold particles.

Human hepatocyte chimeric mouse experiments. Human hepatocytes were transplanted into urokinase-type plasminogen activator-transgenic SCID mice(uPA$^{+/+}$ SCID$^{+/+}$) as described previously (33). All mice received hepatocyte transplants from the same donor. Human hepatocyte chimeric mice, in which liver cells were largely (>90%) replaced with human hepatocytes, were used to reduce the potential influence by mouse-derived mRNA. Human albumin levels in the sera of mice were monitored to evaluate the replacement ratio of the human hepatocytes in the mouse liver. The mice were obtained from Phoenix Bio Co., Ltd. (Hiroshima, Japan). Four mice were divided into two groups. Each group of mice was inoculated with 1×10^6 RNA copies of either purified J6/JFH2/AS HCV particles or JFH-2 patient serum. The HCV RNA titer in inoculated mouse serum was monitored by real-time detection RT-PCR each week after inoculation.

RESULTS

HCV clone from a fulminant hepatitis patient. HCV cDNA was isolated from a fulminant hepatitis patient as described in Materials and Methods (clone JFH-2) (15). HCV RNA was detected by RT-PCR in the patient's serum during the acute phase (Fig. 1). All viral markers of the other hepatitis viruses were negative. By the phylogenetic analysis, the JFH-2 clone was clustered into genotype 2a (Fig. 2). JFH-2 exhibits 87.6%, 89.0%, and 88.9% nucleotide homology with JFH-1, J6CF, and JCH-1, respectively, and 90.6%, 91.8%, and 91.8% amino acid homology with JFH-1, J6CF, and JCH-1, respectively (Table 2). The JFH-1 strain is cell culture replication-competent, but the J6CF and JCH-1 strains are incompetent. However, the homology data for nucleotide and amino acid sequences are very similar in both the structural and nonstructural regions. We also mapped the

TABLE 2 Percent homology between JFH-2 and other genotype 2a strains

Region	JFH-2 nucleotide profile				JFH-2 amino acid profie			
	Lenght (nt)[a]	% Identity vs strain:			Length (aa)[b]	% Amino acid identity vs strain:		
		JFH-1	J6CF	JCH-1		JFH-1	J6CF	JCH-1
Entire genome	9683	87.60	88.98	88.88	3033	90.64	91.79	91.79
UTR[c]	576	96.35	98.61	96.88	NA[d]			
Structural	2439	86.14	87.90	86.51	813	89.30	89.54	88.56
Nonstructural	6663	87.44	88.59	89.12	2220	91.13	92.61	92.97
5′ UTR	340	98.82	99.71	99.71	NA			
Core	573	91.80	93.02	91.97	191	92.15	95.29	92.15
E1	576	87.50	88.89	89.06	192	90.10	92.19	89.58
E2-p7	1290	83.02	85.19	82.95	430	87.67	85.81	86.51
NS2	651	84.18	85.87	89.09	217	87.56	88.02	91.24
NS3	1893	87.64	88.54	89.33	631	92.87	94.61	94.45
NS4A	162	88.27	88.27	88.27	54	96.30	92.59	94.44
NS4B	783	89.91	90.04	89.14	261	96.93	97.32	96.55
NS5A	1398	83.48	85.98	85.48	466	82.83	86.70	86.48
NS5B	1776	90.37	91.10	91.84	591	94.08	94.75	95.43
3′ UTR	236	92.80	97.03	92.80	NA			

[a] nt, nucleotides.
[b] aa, amino acids.
[c] UTR, 5′ UTR plus 3′ UTR.
[d] NA, not applicable.

positions of different amino acid sequences of each strain (Fig. 3A). The E2 and NS5A regions are more variable than other regions (Fig. 3A and Table 2); however, it is difficult to find particular mutation positions or regions specific for the JFH-2 strain.

Subgenomic replicon analysis of the JFH-2 clone. Interestingly, some parts of the viral cDNA sequences in the JFH-2 viral genome were a mixture of different sequences, especially in the NS3 region. By the cloning analysis, we found two major se-

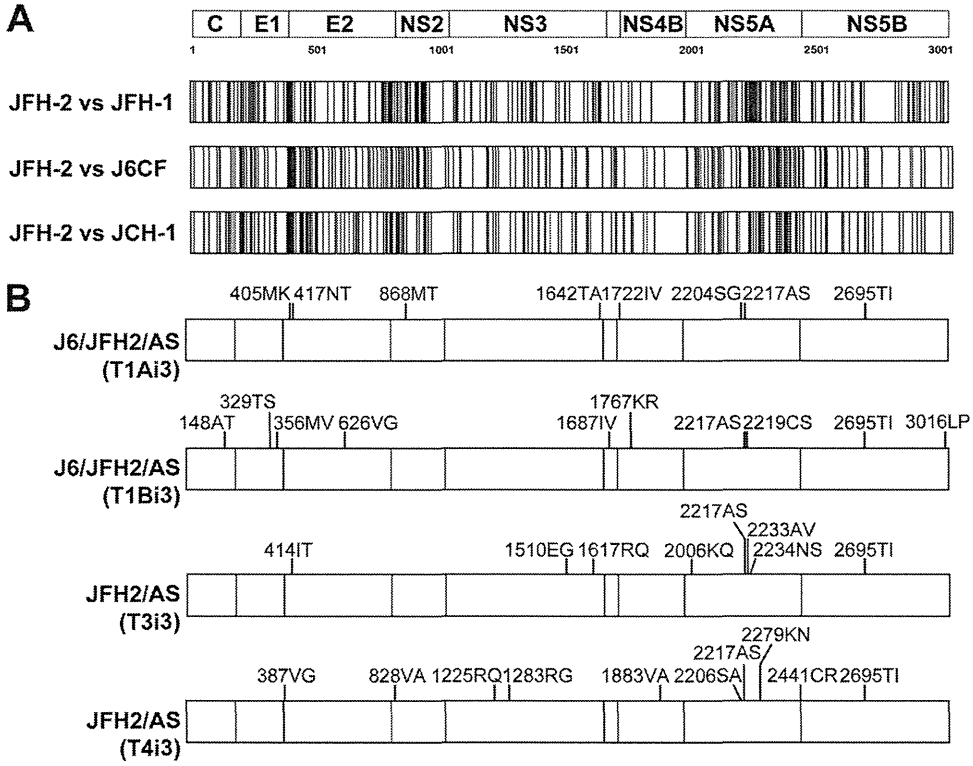

FIG 3 Maps of amino acid sequences among genotype 2a HCV strains and mutations found in the cell culture-adapted viruses. (A) Amino acid sequences of the entire open reading frame (3,033 amino acids) of JFH-1, JFH-2, J6CF (accession numbers AB047639, AB690461, and AF177036, respectively), and JCH-1 strains were compared. The positions of different sequences are indicated by vertical lines. (B) Virus genome sequences were determined in the T1Ai3 and T1Bi3 culture media of the J6/JFH2/AS virus-inoculated cells or T3i3 and T4i3 culture media of the JFH2/AS virus-inoculated cells, as described in the text. Amino acid mutations are indicated with their positions and residues.

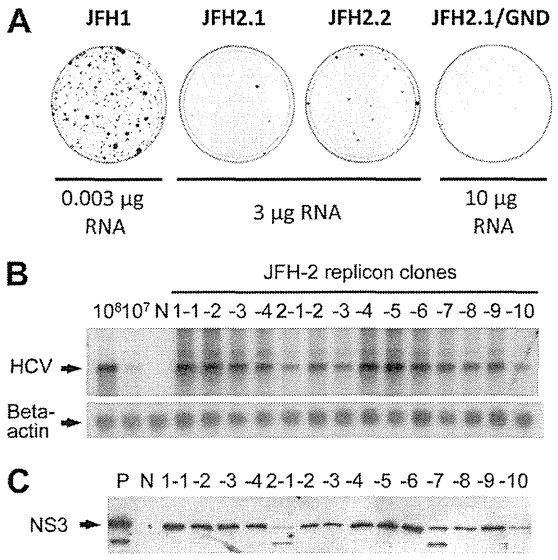

FIG 4 G418-resistant colony formation of JFH-1 and JFH-2 replicons and analysis of JFH-2 replicon cells. (A) Subgenomic RNAs were synthesized *in vitro* by using pSGR-JFH1, pSGR-JFH2.1, pSGR-JFH2.2, and pSGR-JFH2.1/GND as templates. Transcribed subgenomic RNAs were electroporated into HuH-7 cells, and cells were cultured with G418 for 3 weeks before being stained with crystal violet. JFH-1 subgenomic RNA (0.003 μg), 3 μg of JFH-2.1 and JFH-2.2 subgenomic RNA, and 10 μg of JFH-2.1/GND subgenomic RNA were transfected into HuH-7 cells. Experiments were performed in triplicate, and representative staining examples are shown. (B) Northern blot analysis. Total cellular RNA isolated from each of four SGR-JFH2.1 clones (1-1 to 1-4) and 10 SGR-JFH2.2 clones (2-1 to 2-10) was analyzed by using a random-primed DNA probe to detect replicon RNA. Isolated total cellular RNA (4 μg) was separated by denatured agarose gel electrophoresis. After electrophoresis, HCV- and beta-actin-specific RNAs were detected by Northern blot analysis with random-primed DNA probes specific to HCV and beta-actin sequences. Arrows indicate replicon RNA or beta-actin mRNA. (C) Western blot analysis. Cell lysates were prepared from four SGR-JFH2.1 clones (1-1 to 1-4) and 10 SGR-JFH2.2 clones (2-1 to 2-10). The NS3 proteins were detected with rabbit anti-HCV NS3 antibody. Positive-control (P) and negative-control (N) cell lysates were obtained from JFH-1 replicon cells and naive HuH-7 cells.

quences in the JFH-2 viral genome. One sequence contained alanine and isoleucine (AI) at amino acid positions 1204 and 1205, and the other contained methionine and leucine (ML) at the same positions. We referred to these viral genomes containing AI or ML as JFH-2.1 or JFH-2.2, respectively. From the cloning analysis of PCR products, JFH-2.1 populated 19 of 32 clones (59%), and JFH-2.2 populated 13 of 32 clones (41%). To analyze the replication efficiency of the JFH-2 clone, we thus constructed two subgenomic replicon constructs, pSGR-JFH2.1 and pSGR-JFH2.2, as pSGR-JFH1 (11). Synthesized replicon RNAs of JFH-2.1 and JFH-2.2 were independently transfected by electroporation into HuH-7 cells. The transfected cells were then grown for 3 weeks in selection culture that contained 1 mg/ml of G418. Several colonies survived the selection culture, as illustrated by crystal violet staining (Fig. 4A). The JFH2.1/GND replication-incompetent control RNA-transfected cells did not form any colonies, even when 10 μg of RNA was transfected. The colony formation efficiencies of the JFH-2.1 and JFH-2.2 replicons were 0.94 ± 0.54 and 6.43 ± 3.39 CFU/μg RNA, respectively, which were substantially lower than the colony formation efficiency of the JFH-1 subgenomic replicon ($5.32 \times 10^4 \pm 5.02 \times 10^4$ CFU/μg RNA) (11). Four colonies of the JFH-2.1 replicon and 10 colonies of the JFH-2.2 replicon were cloned and expanded for further analysis. Replicon RNA was isolated from each replicon cell clone, and the HCV RNA titer and sequence of the replicon genome were determined (Table 3). The average HCV RNA titer in replicon cell clones was determined by real-time RT-PCR detection as $(8.70 \pm 4.94) \times 10^7$ copies/μg of RNA. The size and amount of the replicon RNA in the replicon cells were confirmed by Northern blot analysis (Fig. 4B). We also detected NS3 protein in each clone of replicon cells by Western blot analysis (Fig. 4C). NS3 proteins were mainly found at approximately 70-kDa by polyclonal anti-NS3 antibody; however, an additional signal was also detected at a smaller molecular size in some replicon cells, including the positive-control JFH-1 replicon cells.

Next, we determined the sequences of replicating RNA in each replicon cell clone. Most of the clones, except replicon clone 2.2-8, had at least one nonsynonymous mutation (Table 3). We found nonsynonymous mutations in the NS3, NS5A, and NS5B regions, and three mutations were common among the different replicon genomes. Among the mutations found in the NS3 region, both 1547FL and 1614CW were found in two different replicon cells, and the 1651TN mutation was found in five replicon cells. The 2280QR mutation in NS5A was found in three replicon cells. 2217AS and 2222HQ, which are located in the interferon sensitivity-determining region (ISDR), were each found in a single replicon cell (8). To determine the adaptive effect of these mutations (Fig. 5A), we inserted these mutations (listed in Table 3), except for 1204MK, into pSGR-JFH2.1 and tested the colony formation efficiency of the mutant replicons. The 1204MK mutation was not tested since methionine at amino acid position 1204 was specific for the JFH2.2 sequence. As shown in Fig. 5B, 1547FL, 1614CW, 1651TN, 2222HQ, and 2280QR had weak to moderate adaptive effects for colony formation. Interestingly, the 2217AS mutation in the ISDR strongly enhanced the colony formation to approximately 3×10^4 times that of the parental JFH2.1 replicon (Fig. 5B). We further tested these adaptive mutations in the luciferase reporter replicon format, as described previously (12). SGR-JFH2.1 with the 2217AS construct exhibited significant replication compared to JFH2.1/GND, which is the replication-incompetent negative control. However, other constructs showed no evidence of replication in the transient replication assay (Fig. 5C).

Full-length HCV replication. The 2217AS mutation substantially enhanced RNA replication of the JFH-2.1 subgenomic replicon compared with other mutations. We examined whether a full-length JFH-2 HCV clone with the 2217AS mutation could produce infectious virus. In our previous study, we constructed the J6/JFH1 chimeric construct by replacement of the 5′ untranslated region to the p7 region (EcoRI-BclI) of J6 (1), and we found that J6/JFH1 produces a larger amount of infectious virus in the culture medium (3). We thus used the structural region of the J6CF clone and the NS2 region of the JFH-1 clone from a J6/JFH-1 chimeric virus construct and fused it to the NS3 to 3′X regions of JFH-2.1 with the 2217AS mutation (plasmid pJ6/JFH2/AS) since it was not clear if the structural and NS2 regions of the JFH-2 strain were functionally intact (Fig. 6A). Full-length viral RNA was synthesized from linearized pJ6/JFH2/AS and electroporated into Huh-7.5.1 cells. After two independent transfections, the transfected cells were divided into sub-cell lines to form a total of four sub-cell lines (T1A, T1B, T2A, and T2B). All four sub-cell lines were serially passaged, and HCV core protein, RNA, and infectivity levels in the culture supernatant were monitored (Fig.

TABLE 3 Mutations and RNA titer of the JFH-2 replicon cell clones

Replicon clone	Nucleotide		Amino acid		Region	Replicon titer (no. of copies/μg of RNA)
	Mutation	Position	Mutation	Position		
2.1-1	A→G	2012	E→G	1109	NS3	1.30E+8
	C→A	3638	T→N	1651	NS3	
2.1-2	T→C	3325	F→L	1547	NS3	1.52E+8
	C→A	3638	T→N	1651	NS3	
2.1-3	A→G	5525	Q→R	2280	NS5A	1.09E+8
	A→G	7155	None		NS5B	
2.1-4	C→A	3638	T→N	1651	NS3	1.41E+8
	A→G	7795	None		3′ UTR	
2.2-1	C→G	3528	C→W	1614	NS3	2.33E+7
2.2-2	G→T	5335	A→S	2217	NS5A (ISDR)	3.57E+7
2.2-3	C→G	919	None		*neo*	3.35E+7
	C→A	5352	H→Q	2222	NS5A (ISDR)	
2.2-4	C→A	1223	None		EMCV-IRES[a]	1.05E+8
	C→A	2115	None		NS3	
	G→T	6243	K→N	2519	NS5B	
2.2-5	C→A	3327	F→L	1547	NS3	1.67E+8
2.2-6	T→C	625	None		*neo*	1.09E+8
	C→A	3638	T→N	1651	NS3	
	A→G	5525	Q→R	2280	NS5A	
	T→A	5754	None		NS5A	
	G→A	5803	G→S	2373	NS5A	
2.2-7	C→G	3528	C→W	1614	NS3	6.25E+7
2.2-8	None		None			5.31E+7
2.2-9	C→G	3638	T→N	1651	NS3	6.71E+7
	G→A	5269	A→T	2195	NS5A	
	A→G	5525	Q→R	2280	NS5A	
2.2-10	T→A	2297	M→K	1204	NS3	2.95E+7
	A→G	7815	None		3′ UTR	

[a] EMCV-IRES, encephalomyocarditis virus internal ribosome entry site.

6B and C and Table 4). At the first cell passage, the HCV core protein levels were approximately 300 fmol/liter, and the infectivities were very low. Secreted HCV core protein levels decreased in all of the passaged cells until 25 days after the transfection. However, HCV core protein secretion of passaged T1A cells began to increase from 30 days after transfection. Subsequently, increased core protein secretion was also observed in other passaged cells although at different time points (Fig. 6B and Table 4). The maximum core protein levels in the medium were up to 9,241 fmol/liter in T1B cells at day 75 posttransfection. Infectivity detected in the culture medium was also first increased in T1A, and similar increases were observed with other passaged cells at later time points. Furthermore, specific infectivity (infectivity/HCV RNA or infectivity/HCV core protein) was also higher than in the initial culture medium (Table 4). The passaged cells were immunostained with anti-core monoclonal antibody (Fig. 6D). At 4 weeks after transfection, only a few cells were positive in all four sub-cell lines. However, the number of positive cells increased from 8, 12, 18, or 14 weeks after transfection in T1A, T1B, T2A, or T2B cells, respectively. These results indicate that phenotypic change occurred in the replicating virus after the serial passages of the transfected cells. Before this phenotypic change, the replicating viruses were not able to secrete significant amounts of infectious virus particles due to an unknown defect in infectious virus particle formation or secretion. After the phenotypic change, the robust core protein secretion might have been caused by changes in the efficiency of infectious virus production or secretion. To compare the virus characteristics before and after the phenotypic change, we analyzed T1A culture medium from 5 days, 8 weeks, and 11 weeks posttransfection by density gradient assay (Fig. 6E). The day 5 medium showed a broad density profile both of core protein and HCV RNA, and infectivity was not detected. Interestingly, the peaks of HCV core protein and RNA at around 1.15 mg/ml density became higher at 8 weeks and had a further increase at 11 weeks. Broader minor peaks at the lighter density remained small at week 11. The infectivity peak also became higher at 8 and 11

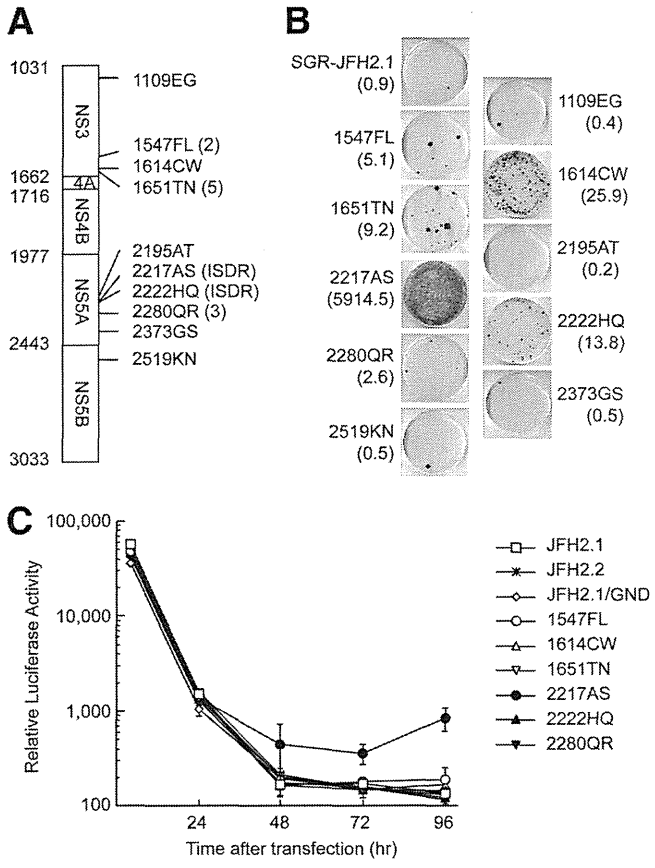

FIG 5 Analysis of the effect on colony formation and transient replication efficiency of mutations detected in replicon cell clones. (A) The box indicates the open reading frame of JFH-2 replicon and amino acid sequences at positions 1031 and 3033 (numbering by full-length JFH-2). The numbers on the left side of the box show the starting position of each protein, with the exception of 3033, which is the end position of NS5B. The numbers with the lines on the right side indicate the mutations introduced in the replicon constructs. 1547FL, 1651TN, and 2280QR mutations were found in 2, 5, and 3 replicon clones, respectively (Table 3). 2217AS and 2222HQ mutations were found in the ISDR (Table 3). (B) Each amino acid mutation found in the replicon genome was introduced into the pSGR-JFH2.1 replicon construct, and colony formation of the JFH2.1 replicon with the wild-type sequence (SGR-JFH2.1) and other mutations was tested. Briefly, transcribed RNA (5 μg) was transfected into HuH-7 cells, and cells were cultured for 3 weeks before being stained with crystal violet. The numbers in the parentheses show the colony formation efficiency (CFU/μg of RNA) of the replicon constructs. (C) Transient replication of JFH-2 subgenomic replicon. HuH-7 cells were transfected with the transcribed RNA from pSGR-JFH2.1/Luc, pSGR-JFH2.2/Luc, pSGR-JFH2.1/Luc/GND (replication-incompetent control), and pSGR-JFH2.1/Luc constructs with adaptive mutations (1547FL, 1614CW, 1651TN, 2217AS, 2222HQ, and 2280QR). Transfected cells were harvested at the indicated time points and at 4 h posttransfection. Relative luciferase activity (arbitrary units) was measured in the cell lysate. Assays were performed in triplicate, and data are presented as means ± standard deviations. The background signal of the luciferase measurement was 129.4 ± 27.4 units.

weeks after transfection. Interestingly, this density profile at 11 weeks posttransfection was quite similar to that of JFH-1 or the J6/JFH1 chimera, as previously described (21, 38). Furthermore, virus-like particles were visualized in the concentrated culture medium by electron microscopic analysis, whereas only unstructured aggregates were found with the mock-transfected control (Fig. 7, left panel; also data not shown). An aliquot of the culture medium was used for immunoelectron microscopy with an E2-specific antibody (AP33), and gold-labeled spherical structures were detected (Fig. 7, middle panel). The overall diameter of the structures (50 to 65 nm) is compatible with the predicted size of HCV.

Characterization of cell culture-adapted J6/JFH2/AS virus. During the serial passages of the transfected cells, the J6/JFH2/AS virus adapted to produce more infectious viruses in the cell culture. We next compared the adapted J6/JFH2/AS virus (T1B cells at day 75 posttransfection) with the J6/JFH1 virus. Huh-7.5.1 cells were inoculated with the viruses at a multiplicity of infection (MOI) of 0.03. The core protein production levels in both the infected cells and the culture medium were increased with similar kinetics after the virus infection, although at lower levels for J6/JFH2/AS virus than J6/JFH1 virus (Fig. 8A). We also tested the neutralization of the infection of these viruses by using mouse anti-CD81 monoclonal antibody and anti-HCV human IgG purified from HCV carrier serum (Fig. 8B). Both antibodies clearly inhibited the infectivity of inoculated virus to Huh-7.5.1 cells. Thus, the J6/JFH2/AS and J6/JFH1 viruses appeared to share similar infection pathways.

Adaptive mutations in the cell culture-adapted J6/JFH2.2/AS virus. We determined the full-length sequence of the HCV genome in the culture medium of T1A and T1B sub-cell lines at 75 days posttransfection by directly sequencing the amplified virus cDNA. We found the following nonsynonymous mutations, in addition to 2217AS, in the viral genomes: 1342ST in NS3 and 2219CR in NS5A of T1A and 148AT in the core protein, 2219CS in NS5A, and 2695TI and 3016LP in NS5B of T1B. These mutations were introduced into the J6/JFH2.2/AS cDNA, and synthetic RNA was transfected into Huh-7.5.1 cells. However, robust virus production was not observed at an early time point after transfection (data not shown). Because the important adaptive mutations might still not be detected in the virus population, we decided to concentrate on the dominant virus population and fix the important mutations in T1A and T1B virus by serial virus passages. We thus repeatedly inoculated naive Huh-7.5.1 cells three times with J6/JFH2/AS virus at a low MOI and harvested the virus when the virus titer plateaued. We sequenced the full-length genome of virus in the culture medium after the third inoculation (T1Ai3 or T1Bi3) and found the following nonsynonymous mutations: 405MK and 417NT in E2, 868MT in NS2, 1642TA in NS3, 1722IV in NS4B, 2204SG in NS5A, and 2695TI in NS5B of T1Ai3; and 148AT in the core protein, 329TS and 356MV in E1, 626VG in E2, 1678IV in NS4A, 1767KR in NS4B, 2219CS in NS5A, and 2695TI and 3016LP in NS5B of T1Bi3 (Fig. 3B). We then introduced these mutations into pJ6/JFH2/AS to construct pJ6/JFH2/AS/mtT1A and pJ6/JFH2/AS/mtT1B. Synthetic RNAs produced from both of the mutation-containing plasmids and control plasmids were transfected into Huh-7.5.1 cells. After the transfection, core proteins were secreted into the culture medium at levels similar to those of JFH-1 RNA-transfected cells but at lower levels than J6/JFH1 RNA-transfected cells (Fig. 9A). HCV RNA levels in the culture medium of J6/JFH2/AS/mtT1A (mtT1A) and J6/JFH2/AS/mtT1B (mtT1B) RNA-transfected cells were less than those in cells transfected with either or JFH-1 J6/JFH1 RNA (Fig. 9B). This discrepancy may be due to the lower detection efficiency of the JFH-1 core protein in the immunoassay, as reported previously (31). Infectivity in the culture medium was also determined. Interestingly, higher infectious titers were detected in the culture medium of the J6/JFH2/AS/mtT1A and J6/JFH2/AS/mtT1B

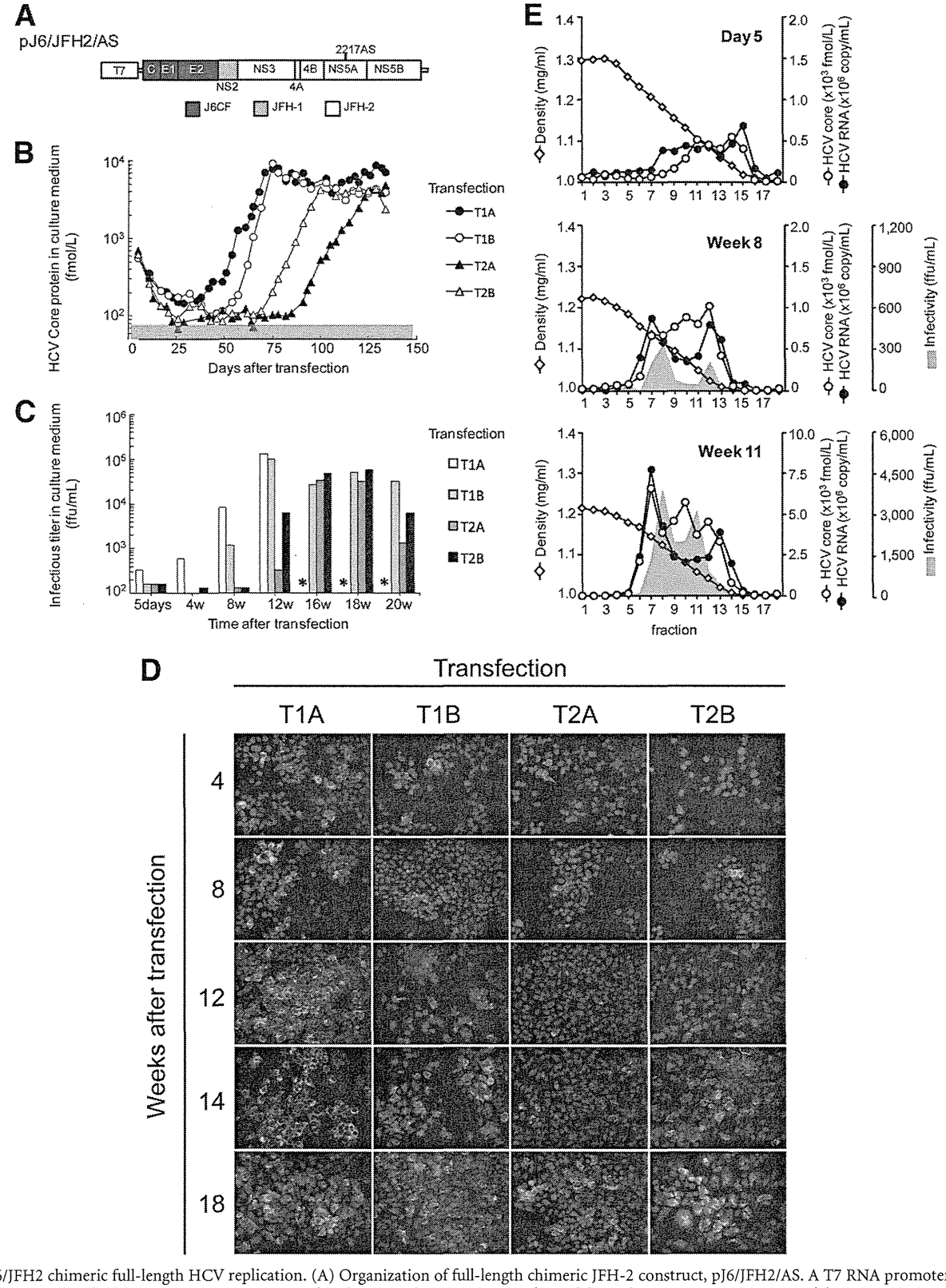

FIG 6 J6/JFH2 chimeric full-length HCV replication. (A) Organization of full-length chimeric JFH-2 construct, pJ6/JFH2/AS. A T7 RNA promoter is located upstream of the 5′ end of the HCV cDNA construct. The 5′ UTR and NS2 region are derived from the JFH-1 strain. Regions of the core protein to E2/p7 are derived from the J6CF strain. The 2217AS adaptive mutation is introduced. (B) Huh-7.5.1 cells were transfected with the transcribed RNA from pJ6/JFH2/AS. Two independently transfected cell lines (transfections 1 and 2 [T1 and T2, respectively]) were divided into two passages, resulting in four independently passaged transfected cell lines (T1A, T1B, T2A, and T2B). At each time point, culture medium was harvested and analyzed for the presence of HCV core protein by Lumipulse Ortho HCV Ag (Ortho-Clinical Diagnostics). The gray area indicates values that are below the detection limit. (C) Infectious titers in the culture supernatant of the passaged transfected cells (T1A, T1B, T2A, and T2B) were determined by focus formation assay. After 16 weeks, the culture media from T1A

TABLE 4 Specific infectivity of culture medium after transfection of J6/JFH2/AS RNA

Cell culture medium (no. of days posttransfection)	Infectivity (FFU/ml)	HCV core protein (fmol/liter)	HCV RNA (no. of copies/ml)	Specific infectivity	
				Infectivity/HCV core protein	Infectivity/HCV RNA (10^4)
T1A (5)	3.20E+1	3.57E+2	2.63E+6	0.09	0.12
T1B (5)	1.60E+1	3.07E+2	2.35E+6	0.05	0.07
T2A (5)	1.60E+1	3.13E+2	2.99E+6	0.05	0.05
T2B (5)	1.60E+1	2.63E+2	3.42E+6	0.06	0.05
T1A (82)	1.28E+4	5.47E+3	2.63E+7	2.34	4.87
T1B (82)	9.83E+3	5.98E+3	2.73E+7	1.64	3.61
T2A (120)	3.17E+3	2.47E+3	8.49E+6	1.28	3.73
T2B (120)	5.83E+3	4.51E+3	2.83E+7	1.29	2.06

RNA-transfected cells than in JFH-1 RNA-transfected cells; however, they were lower than in J6/JFH-1 RNA-transfected cells (Fig. 9C).

Transfected cells were serially passaged, and, importantly, both types of transfected cells (J6/JFH2/AS/mtT1A and J6/JFH2/AS/mtT1B RNA) secreted core protein and HCV RNA at high levels, even at the first passage after transfection, and the levels of HCV core protein and RNA were maintained during the passages (Fig. 10A and B). Infectious titers in the medium of the transfected cells were also measured (Fig. 10C). J6/JFH2/AS/mtT1A secreted a higher infectious titer than J6/JFH2/AS/mtT1B although their HCV core protein levels and RNA levels in the culture medium were similar. To confirm the rapid infectious viral production phenotype of these viruses, we inoculated naive Huh-7.5.1 cells with the culture medium of J6/JFH2/AS/mtT1A and J6/JFH2/AS/mtT1B RNA-transfected cells at 8 and 38 days posttransfection at an MOI of 0.01. All of the inoculated cells secreted core protein and HCV RNA with similar kinetics (Fig. 11A and B). The infectious titer was also determined in the culture medium of the infected and passaged cells (Fig. 11C). mtT1B (day 38 posttransfection) showed lower infectivity at 7 days after inoculation; however, substantial infectivity was detected at 13 and 27 days. The culture medium of mtT1A (day 8 and day 38 posttransfection) was harvested at 20 days after inoculation and analyzed by a sucrose density gradient assay, as described above (Fig. 11D). Major peaks of both HCV core protein and RNA were clearly shown at around 1.15 mg/ml, and the subpeaks of HCV core protein were found in lighter fractions. On the other hand, major peaks of infectivity were found at around 1.0 mg/ml. Compared to the data shown in Fig. 6E, the HCV core and RNA levels and infectivity titer are higher in mtT1A (day 8 and day 38 posttransfection) virus. The similar virus characteristics suggested that J6/JFH2/AS/mtT1A and J6/JFH2/AS/mtT1B viruses do not need further adaptations for autonomous expansion in cultured cells. Thus, we established stable cell culture-adapted virus and constructed recombinant cell culture-adapted infectious HCV clones by reverse genetics.

Human hepatocyte-transplanted uPA/SCID mouse experiment. To determine the *in vivo* infectivity of J6/JFH2/AS virus, we inoculated day 75 culture medium of T1B cells containing 1×10^6 RNA copies of purified J6/JFH2/AS HCV particles and original patient serum also containing 1×10^6 RNA copies into human hepatocyte-transplanted uPA/SCID mice. Inoculation of 1×10^6 RNA copies of cell culture-derived J6/JFH1 virus usually results in robust infection for human hepatocyte-transplanted uPA/SCID mice. Two mice were used for each type of inoculum. Human albumin levels in sera of the inoculated mice were more than 3 mg/ml during the experiment, which supported the high replacement ratio of the human hepatocytes in the mouse liver. Both mice inoculated with patient serum became HCV RNA positive 1 week postinoculation and remained positive during the 4-month observation period (Fig. 12). However, the mice inoculated with J6/JFH2/AS virus in culture medium did not become HCV positive after inoculation (Fig. 12). One mouse inoculated with J6/JFH2/AS virus died 16 days after inoculation, and the cause of death was unknown. HCV RNA was not detected at 7, 14, and 16 days postinoculation. The other mouse inoculated with culture medium was also tested every week for serum HCV RNA and remained negative for 56 days after infection. On day 56, this mouse received a second inoculation with the same culture medium. This mouse was monitored for a total of 63 days, but weekly tests for HCV RNA were continuously negative. Thus, the cell culture-adapted virus in the inoculum may be less viable *in vivo* although the virus acquired robust replication capacity in HuH-7 cells.

Full-length JFH-2 construct. We successfully established J6/JFH2/AS-derived cell culture-adapted viruses. Next, we produced a full-length JFH2/AS virus by using the structural region sequence from JFH-2. pJFH2/AS was constructed according to the viral sequence, and an alanine-to-serine mutation was introduced at amino acid position 2217. JFH2/AS RNA synthesized *in vitro* was electroporated into the Huh-7.5.1 cells, as described above. J6/JFH2/AS RNA was also transfected simultaneously and compared. Two groups of independently transfected cells (transfections 3 and 4 [T3 and T4, respectively]) were analyzed for JFH2/AS and J6/JFH2/AS. Interestingly, JFH2/AS RNA-transfected cells be-

cell lines were not tested (*). (D) The passaged transfected cells were stained with anti-core protein monoclonal antibody (2H9) as a primary antibody at the indicated time points. Green, HCV core protein; blue, 4′,6′-diamidino-2-phenylindole (DAPI) staining. (E) Density gradient analysis of culture supernatant from HCV RNA-transfected Huh-7.5.1 cells. Culture supernatants of transfected cell line T1A collected at 5 days, 8 weeks, and 11 weeks posttransfection were cleared by centrifugation and filtration. Each supernatant was overlaid on the stepwise sucrose density gradient (0%, 10%, 20%, 30%, 40%, 50%, and 60% sucrose) and centrifuged for 16 h at 200,000 × *g* at 4°C. Eighteen fractions were collected from the bottom of the tubes, and the concentration of HCV core protein in each fraction was determined by Lumipulse Ortho HCV Ag. The levels of HCV core protein, HCV RNA, and infectivity were determined in each fraction. Infectivity of the samples from day 5 was negative. Open diamond, buoyant density.

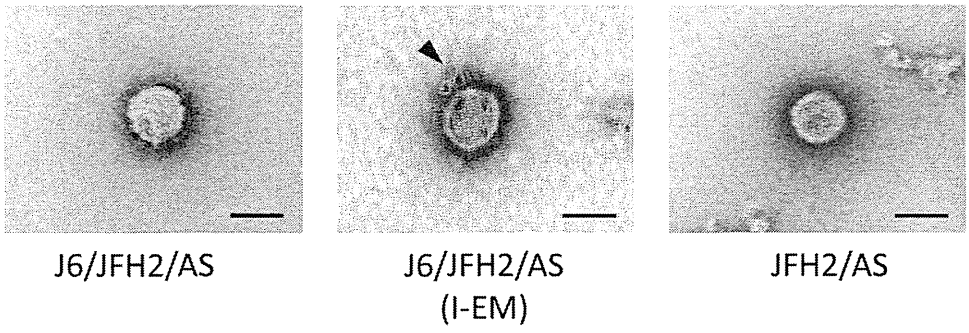

FIG 7 Morphology of JFH-2 virus particles. Negatively stained HCV particles were observed by electron microscopy. J6/JFH-2/AS and JFH2/AS virus particles were purified and observed by electron microscopy by using negative staining. In the middle panel, a J6/JFH-2/AS virus particle was detected by immuno-electron microscopic (I-EM) analysis by using anti-E2 antibody. Arrowhead, gold-labeled antibody. Scale bar, 50 nm.

gan to secrete core proteins earlier than J6/JFH2/AS RNA-transfected cells in this experiment (Fig. 13). Core protein levels were 24,525 and 11,720 fmol/liter in T3 cells at 67 days posttransfection and T4 cells at 63 days posttransfection, respectively. Infectious titers were also determined in the same culture medium at 2.1×10^4 and 4.3×10^4 focus-forming units (FFU)/ml for T3 and T4, respectively. T3 culture medium at day 67 posttransfection was

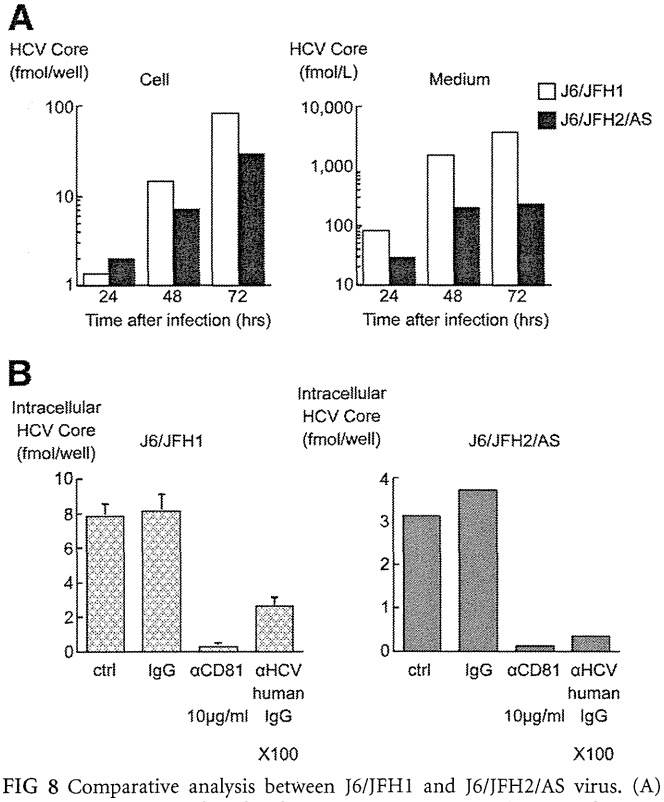

FIG 8 Comparative analysis between J6/JFH1 and J6/JFH2/AS virus. (A) Huh-7.5.1 cells were infected with J6/JFH1 or J6/JFH2/AS virus particles at an MOI of 0.03. HCV core protein production in the inoculated cell lysate and medium was measured at the indicated times. Assays were performed in duplicate, and the average data are represented. (B) Infection with J6/JFH1 and J6/JFH2/AS virus particles was inhibited by adding antibodies to the reaction mixtures. Assays were performed three times independently, and data are presented as means ± standard deviations. Normal human IgG and anti-CD81 monoclonal antibody and anti-HCV human IgG at the indicated concentrations were used. Ctrl, control.

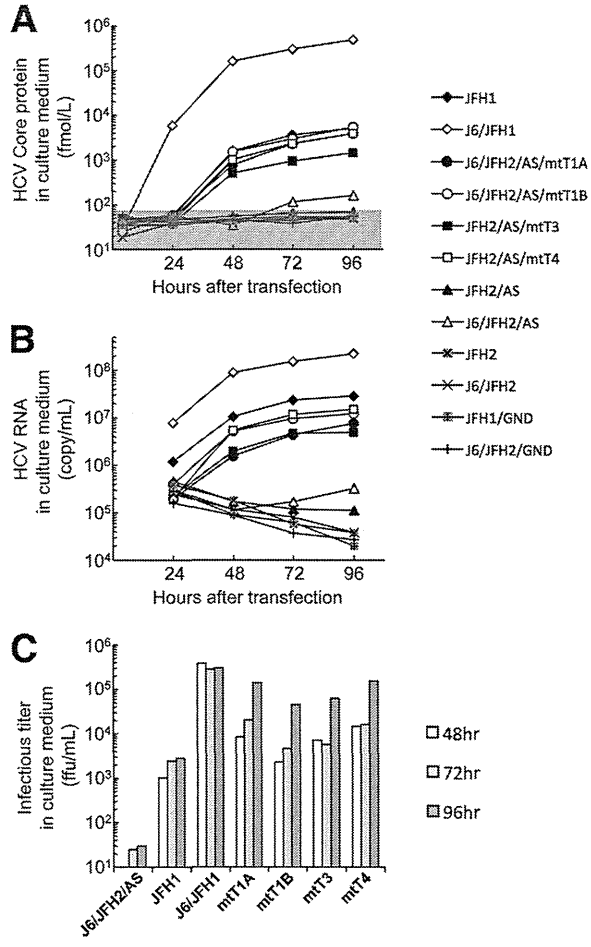

FIG 9 Transient virus production assay of J6/JFH2- and JFH2-related constructs with Huh-7.5.1 cells. Full-length HCV RNA was synthesized from the JFH1, J6/JFH1, JFH2, and J6/JFH2 constructs and their derivatives with mutations and transfected into Huh-7.5.1 cells. (A) HCV core protein levels in the culture medium were determined at 4, 24, 48, 72, and 96 h after transfection. The gray area indicates values that are below the detection limit. (B) HCV RNA levels in the culture medium were also determined at 24, 48, 72, and 96 h after transfection. (C) Infectivity in the culture medium was determined by focus formation assay at 48, 72, and 96 h after transfection. Only positively detected data are shown in the figure. All assays in this figure were performed in duplicate, and the average data are represented.

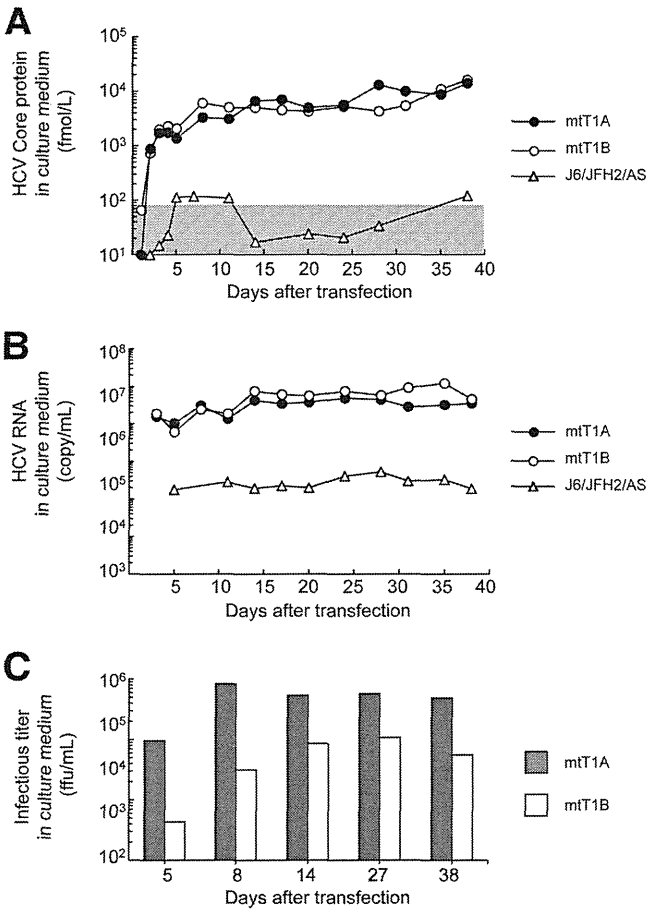

FIG 10 Continuous passage of J6/JFH2/AS cell culture-adapted virus RNA-transfected cells. Full-length HCV RNA was synthesized from the J6/JFH2/AS, J6/JFH2/AS/mtT1A (mtT1A), and J6/JFH2/AS/mtT1B (mtT1B) constructs. RNA-transfected cells were serially passaged until 38 days after transfection, and culture supernatants were harvested at the indicated time points. HCV core protein (A) and HCV RNA (B) levels in the culture media were determined. The data in the gray area were below the detection limit of the assay to detect HCV core protein. (C) Infectivity in the culture medium was determined by focus formation assay at 5, 8, 14, 27, and 38 days after transfection.

also used for electron microscopy analysis. After the density gradient purification, spherical viral particles were detected (Fig. 7, right panel). After the core protein levels plateaued, naive Huh-7.5.1 cells were inoculated with the culture medium, as described above. When the core protein levels plateaued again after the third inoculation of T3 and T4 cells, we sequenced the viral genome in the culture medium (T3i3 and T4i3, respectively) to determine the adaptive mutation. We found the following nonsynonymous mutations: 414IT in E2, 1510EG and 1617RQ in NS3, 2006KQ, 2233AV and 2234NS in NS5A, and 2695TI in NS5B of T3i3; and 387VG in E1, 828VA in NS2, 1225RQ and 1283RG in NS3, 1883VA in NS4B, 2206SA, 2279KN, and 2441CR in NS5A, and 2695TI in NS5B of T4i3 (Fig. 3B). We introduced these mutations into the pJFH2/AS plasmid (pJFH2/AS/mtT3 and pJFH2/AS/mtT4). Synthesized RNA from pJFH2/AS/mtT3 and pJFH2/AS/mtT4 and the related control plasmids was transfected into Huh-7.5.1 cells. HCV core protein levels, HCV RNA levels, and infectivity were monitored in the culture medium of the transfected cells until 96 h after transfection (Fig. 9A to C). JFH2/AS/mtT3 (mtT3) and JFH2/AS/mtT4 (mtT4) secreted similar levels of HCV core protein, RNA, and infectious virus with J6/JFH2/AS/mtT1A and J6/JFH2/AS/mtT1B. Although JFH2/AS/mtT3 secreted slightly higher levels of HCV core protein and RNA than JFH2/AS/mtT4, the secreted infectious virus titers were similar for both viruses. JFH2/AS/mtT3 and JFH2/AS/mtT4 RNA-transfected cells were also serially passaged, and the HCV core proteins were secreted immediately after transfection (Fig. 14A). However, JFH2 and JFH2/AS RNA-transfected cells did not secrete significant amounts of HCV core protein into the culture medium. HCV RNA levels in the culture medium of the RNA-transfected cells were at similar levels for JFH2/AS/mtT3 and JFH2/AS/mtT4 (around 10^7 copy/ml) (Fig. 14B). Infectivity was also detected as higher than 10^4 FFU/ml even at 3 days after the RNA transfection, and this level of infectious titer was maintained during the cell passages (Fig. 14C). We also analyzed JFH2/AS/mtT3 and JFH2/AS/mtT4 culture media by density gradient assay (Fig. 14D). The density profiles with HCV core protein and RNA levels and infectious titers in the fractions were basically similar to those of J6/JFH2/AS-adapted viruses (Fig. 6E and 11D). Taken together, the results described in this section indicate infectious virus was also recovered from the full-length JFH-2 construct with the 2217AS mutation.

Mechanistic analysis of adaptive mutations introduced in the J6/JFH2/AS and JFH2/AS cell culture-adapted viruses. To elucidate the mechanisms of adaptive mutations discovered in J6/JFH2/AS and JFH2/AS virus genomes, we transfected JFH-2 and J6/JFH2 constructs along with possible control constructs into Huh7-25 cells (2) (Fig. 15), which are CD81 defective. The transfection of JFH-1 RNA into Huh7-25 cells results in infectious HCV production, but there was no reinfection into Huh7-25 cells because the cell surface expression of CD81 is essential for HCV infection (10). HCV core protein levels were measured in the culture medium and cell lysate to monitor virus particle secretion and intracellular virus genome replication, respectively (Fig. 15A and B). JFH2/AS, JFH2, J6/JFH2, JFH1/GND, and J6/JFH2/GND RNA-transfected cells did not show increased levels of intracellular core protein expression. However, other RNA-transfected cells showed increased intracellular core protein expression. The cellular core protein level was especially increased at 72 and 96 h after transfection with J6/JFH2/AS RNA, which suggests a higher replication efficiency than J6/JFH; however, core protein secretion was not detected with J6/JFH2/AS, which suggests defective virus particle formation or secretion. Other adaptive mutations in J6/JFH2/AS/mtT1A and J6/JFH2/AS/mtT1B further increased virus genome replication and core protein secretion. In the case of JFH2/AS RNA transfection, cellular core protein expression was not detected, suggesting a lower replication efficiency than that of J6/JFH2/AS. This lower replication efficiency of JFH2/AS may be due to the presence of different sequences in the region of core protein to NS2. However, core protein expression in the cell lysate and culture medium was detected with both JFH2/AS/mtT3 and JFH2/AS/mtT4 RNA transfection. Thus, adaptive mutations in mtT3 and mtT4 are necessary to increase viral genome replication and efficient core protein secretion. JFH-1 and J6/JFH-1 had intracellular core protein expression levels that were similar and high. From the intracellular core protein data, it is clear that J6/JFH2/AS/mtT1A, J6/JFH2/AS/mtT1B, JFH2/AS/mtT3, and JFH2/AS/mtT4 constructs obtained higher replication capacities by

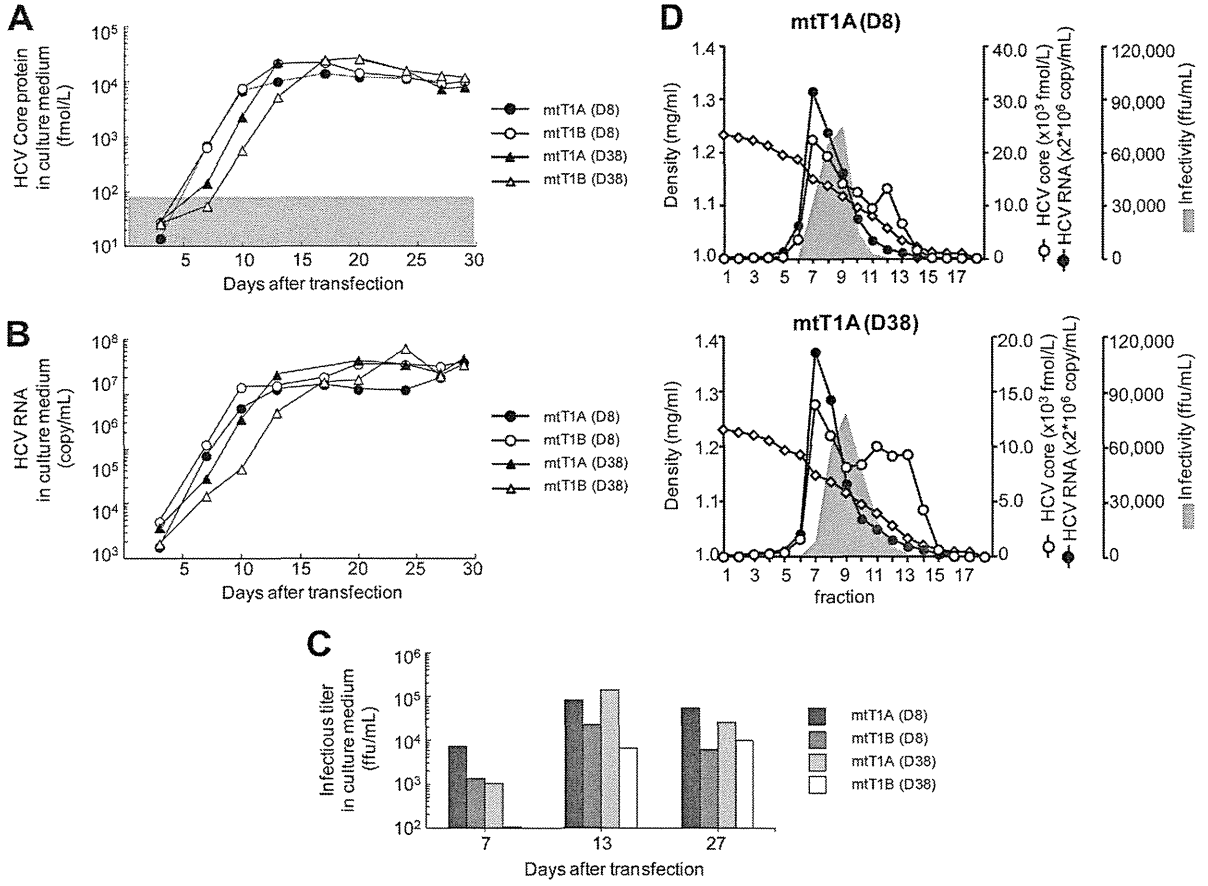

FIG 11 Serial passages of J6/JFH2/AS cell culture-adapted virus infected cells. Naive Huh-7.5.1 cells were inoculated with culture medium of the RNA-transfected cells at an MOI of 0.01. Inoculated cells were serially passaged, and culture supernatants were harvested at the indicated times. HCV core protein (A), HCV RNA (B), and infectivity (C) levels in the culture media were determined. (D) Density gradient analysis of culture supernatant from J6/JFH2/AS/mtT1A cell-culture adapted virus-infected Huh-7.5.1 cells. Culture supernatant of infected Huh-7.5.1 cells with mtT1A (day 8 [D8] D38 posttransfection) was harvested at 20 days after inoculation. Assays were performed as described in the legend of Fig. 6E. Open diamond, buoyant density.

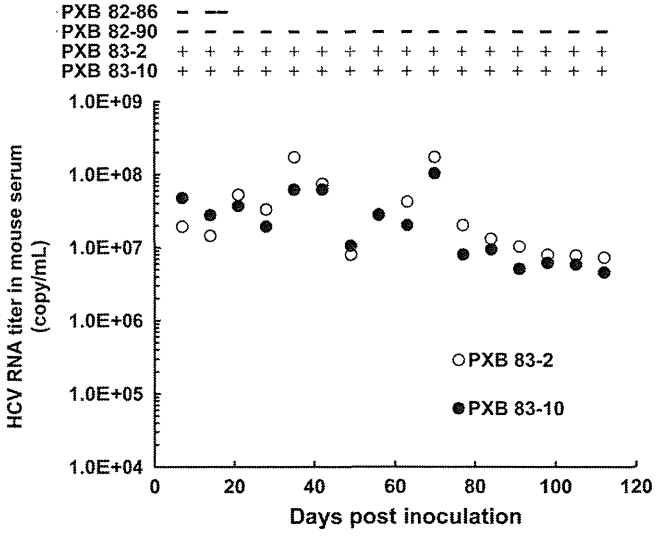

FIG 12 Serum HCV RNA titer in human hepatocyte-transplanted uPA/SCID mice inoculated with JFH-2 serum and cell culture-adapted virus. Mice PXB 82-86 and PXB 82-90 were inoculated with the cell culture-adapted J6/JFH2/AS HCV particles, and mice PXB 83-2 and PXB 83-10 were inoculated with JFH-2 patient serum. Upper and lower panels indicate the results of the RT-PCR and the quantitative detection RT-PCR of HCV RNA in mouse serum, respectively.

adaptive mutations; however, their replication levels are lower than those of JFH-1 and J6/JFH1.

We also analyzed the ratio of extracellular protein to total core protein to analyze the virus secretion efficiency (Fig. 15C). J6/JFH-1 secreted a higher percentage of core protein into culture

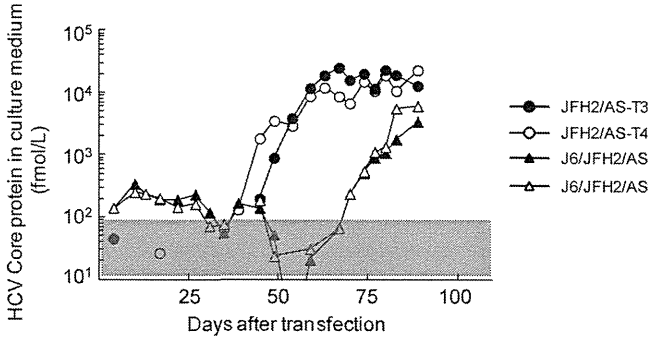

FIG 13 Propagation of a full-length JFH2 virus. Huh-7.5.1 cells were transfected with the transcribed RNA from pJFH2/AS and pJ6/JFH2/AS. Two independently JFH2/AS RNA-transfected cell lines (T3 and T4) were independently passaged. At each time point, culture medium was harvested and analyzed for the presence of HCV core protein.